Supporting Information

Visualization of catalyst dynamics and development of a practical procedure to study complex "cocktail"-type catalytic systems

Alexey S. Galushko[1], Evgeniy G. Gordeev[1], Alexey S. Kashin[1], Yan V. Zubavichus[2] and Valentine P. Ananikov[*1]

[1]*Zelinsky Institute of Organic Chemistry, Russian Academy of Sciences, 119991, Russia, Moscow, Leninsky prospekt, 47*

[2]*Boreskov Institute of Catalysis SB, Russian Academy of Sciences, 630090, Russia, Novosibirsk, Lavrentiev Ave., 5*

E-mail: val@ioc.ac.ru; http://AnanikovLab.ru

Contents

S1. Reaction systems for the formation of metallic nanoparticles

Table S1. Selected ligands and metals for nanoparticles

Entry	Metal	Ligand	Deposition conditions
1	Pd from $Pd_2dba_3{\cdot}CHCl_3$	-	Method A
2	Pd from $Pd_2dba_3{\cdot}CHCl_3$	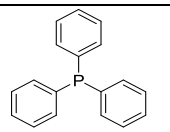 Triphenylphosphine	
3	Pd from $Pd_2dba_3{\cdot}CHCl_3$	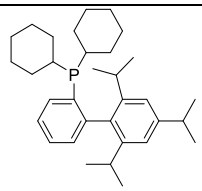 Buchwald ligand	
4	Pd from $Pd_2dba_3{\cdot}CHCl_3$	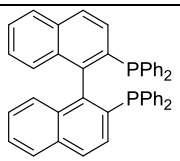 BINAP	
5	Pd from $Pd_2dba_3{\cdot}CHCl_3$	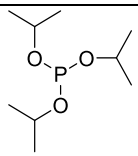 Triisopropyl phosphite	
6	Pd from $Pd_2dba_3{\cdot}CHCl_3$	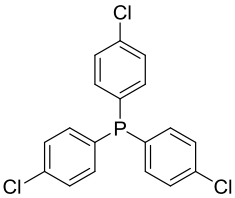 Tris-(4-chlorophenyl)phosphine	
7	Pd from $Pd_2dba_3{\cdot}CHCl_3$	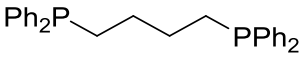 DPPB	
8	Pd from $Pd_2dba_3{\cdot}CHCl_3$	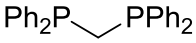 DPPM	
9	Pd from $Pd_2dba_3{\cdot}CHCl_3$	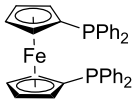 DPPF	
10	Pd from $Pd_2dba_3{\cdot}CHCl_3$	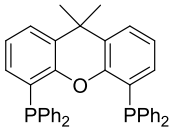 XANTPHOS	

11	Cr from $Cr_2(acac)_3$	-	Method B
12	Co from $CoCl_2 \cdot 6H_2O$	-	
13	Ag from $AgNO_3$	-	
14	Ni from $Ni(OAc)_2 \cdot 4H_2O$	-	
15	Cu from $Cu(OAc)_2$	-	
16	Pd from $Pd(OAc)_2$	-	
17	Cd from $Cd(acac)_2$	-	
18	Ir from $IrCl_4 \cdot H_2O$	-	
19	Ru from $RuCl_3$	-	
20	Rh from $RhCl_3 \cdot H_2O$	-	

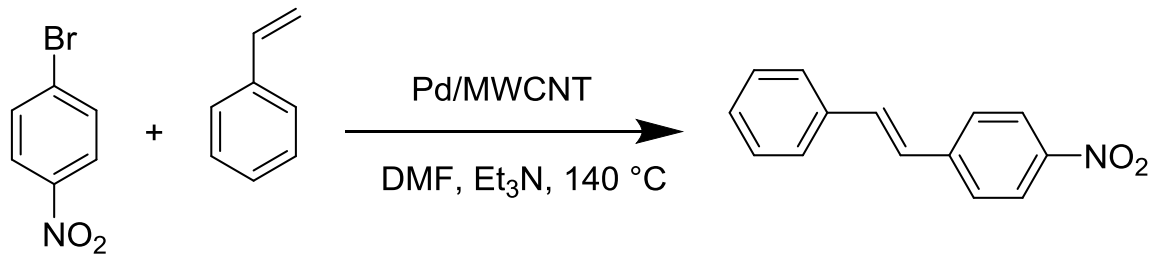

Scheme S1. Heck reaction with heterogeneous catalyst pre-cursor. A test tube with magnetic stir bar was loaded with 1-bromo-4-nitrobenzene (202 mg, 1.0 mmol, Sigma-Aldrich, 99%), styrene (115 μL, 1.0 mmol, Acros Organics, 99%), triethylamine (167 μL, 1.2 mmol, Acros Organics, 99%), 10.6 mg of 1 wt.% Pd/MWCNT and 4 mL of DMF. The reaction mixture was stirred for 6 h at 140 °C and analyzed by ^{1}H NMR.

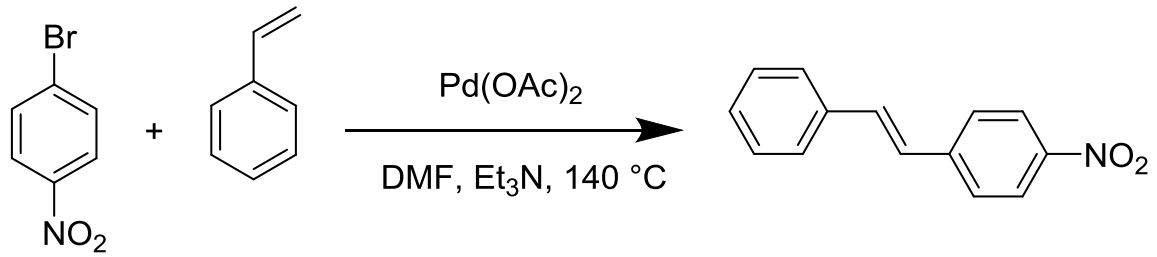

Scheme S2. Heck reaction with homogeneous catalyst pre-cursor. A test tube with magnetic stir bar was loaded with 1-bromo-4-nitrobenzene (202 mg, 1.0 mmol, Sigma-Aldrich, 99%), styrene (115 μL, 1.0 mmol, Acros Organics, 99%), triethylamine (167 μL, 1.2 mmol, Acros Organics, 99%), 2.2 mg of $Pd(OAc)_2$ and 4 mL of DMF. The reaction mixture was stirred for 1 h at 140 °C and analyzed by ^{1}H NMR.

S2. Step by step overview of the «nanofishing» approach

See also video movie in the Supporting Information.

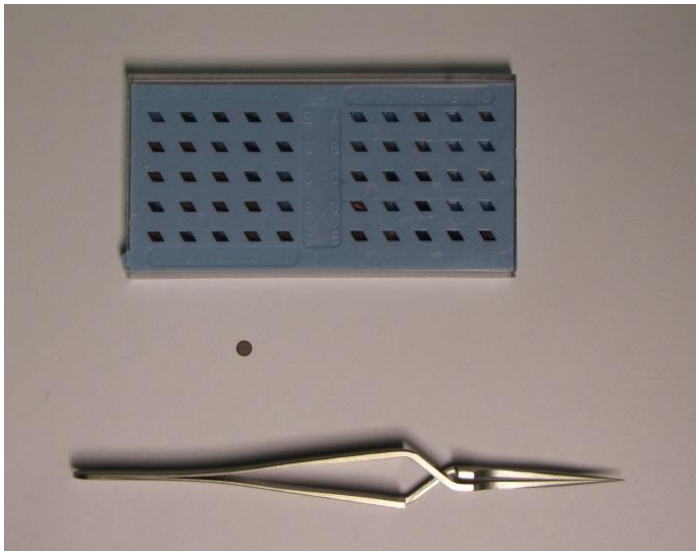

Picture 1.
Cassette for the storage of copper grids for TEM.
A copper grid.
Reverse tweezers.

Picture 2.
A solution comprising nanoparticles.
Reverse action tweezers with the copper grid.

Picture 3.
Deposition of nanoparticles on the carbon-coated surface of the grid by immersion (followed by sample washing in the same manner).

Picture 4.
Air-drying of the sample at room temperature.

S3. Advanced 3D-printed sample holder

Picture 1.
A solution comprising nanoparticles. Advanced 3D-printed sample holder with a grid.

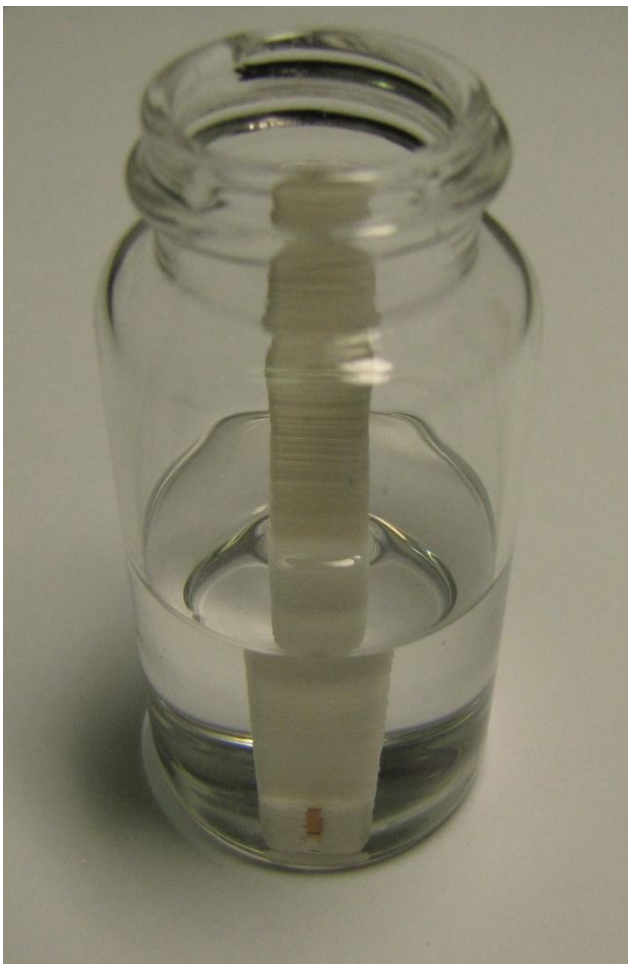

Picture 2.
Deposition of nanoparticles on the carbon surface of the grid by immersion (followed by sample washing in the same manner).

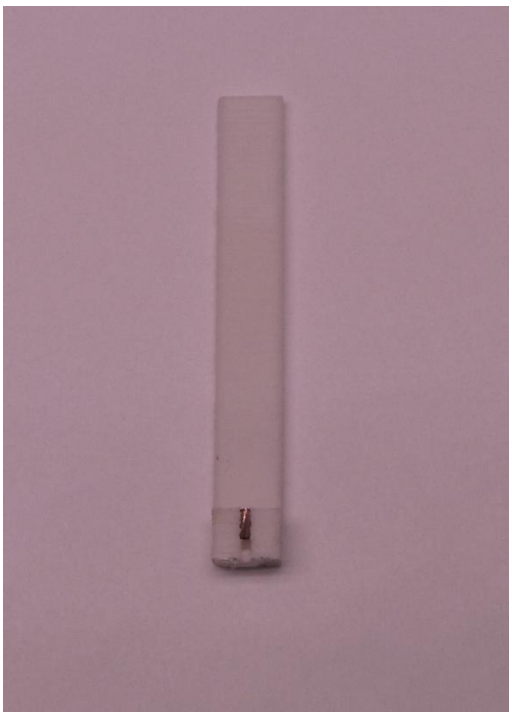

Picture 3.
Air-drying of the sample at room temperature.

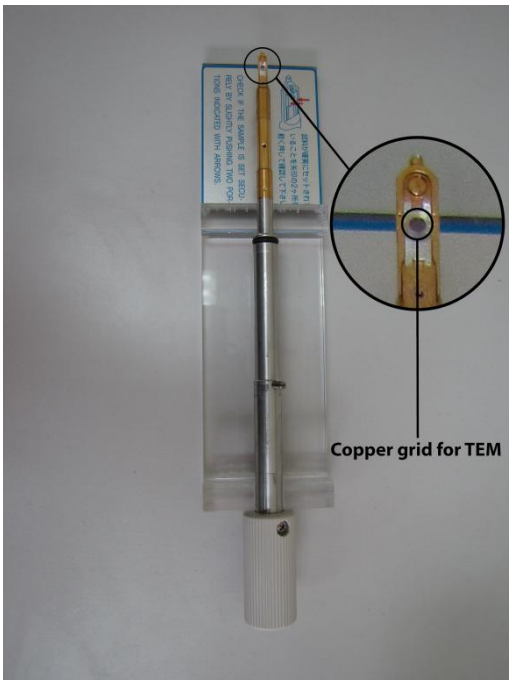

Picture 4.
Loading the sample in a holder for transmission electron microscopy (common step for all nanoparticle capture options)

S4. Palladium nanoparticles formed from Pd_2dba_3 in chloroform solutions

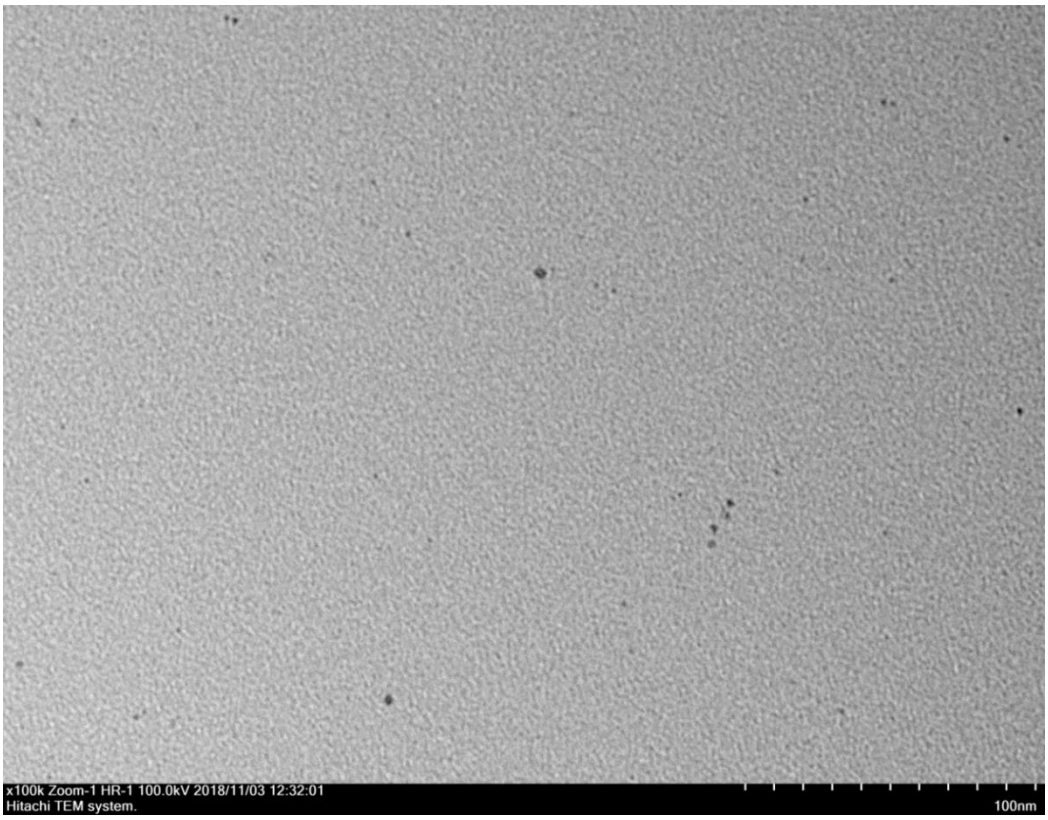

Figure S1. TEM image of palladium nanoparticles formed by Method A in the absence of ligands. 100k magnification.

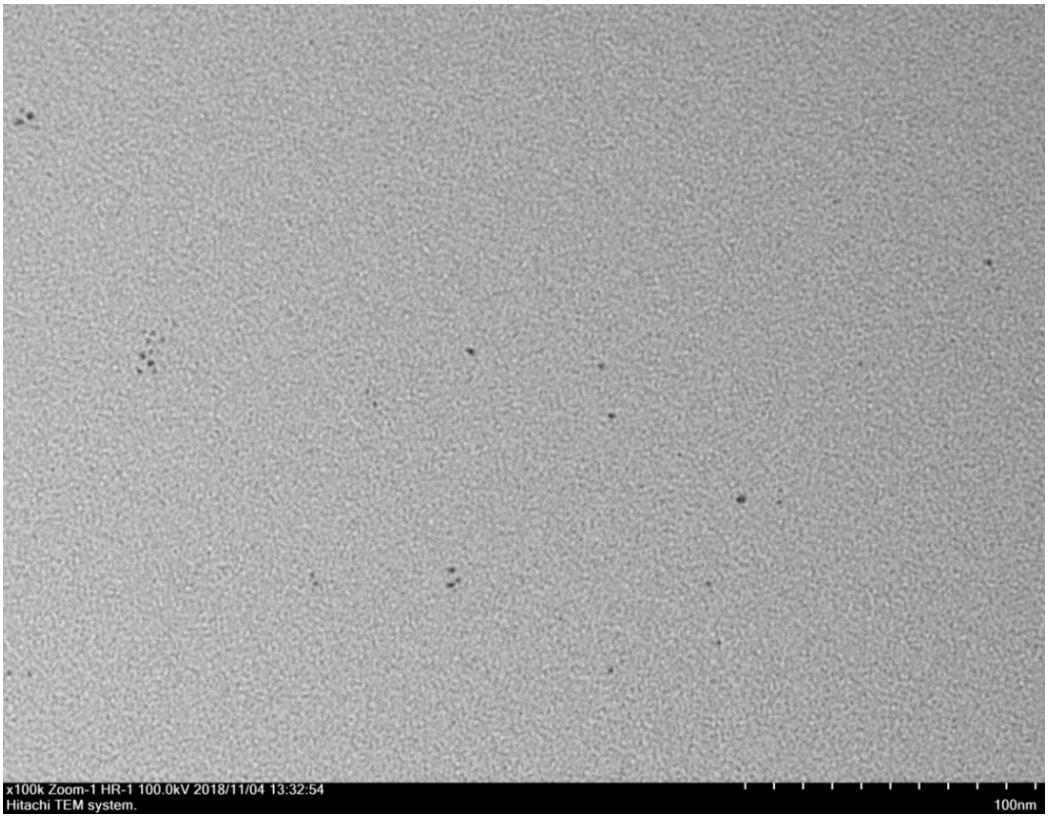

Figure S2. TEM image of palladium nanoparticles formed by Method A in the presence of triphenylphosphine. 100k magnification.

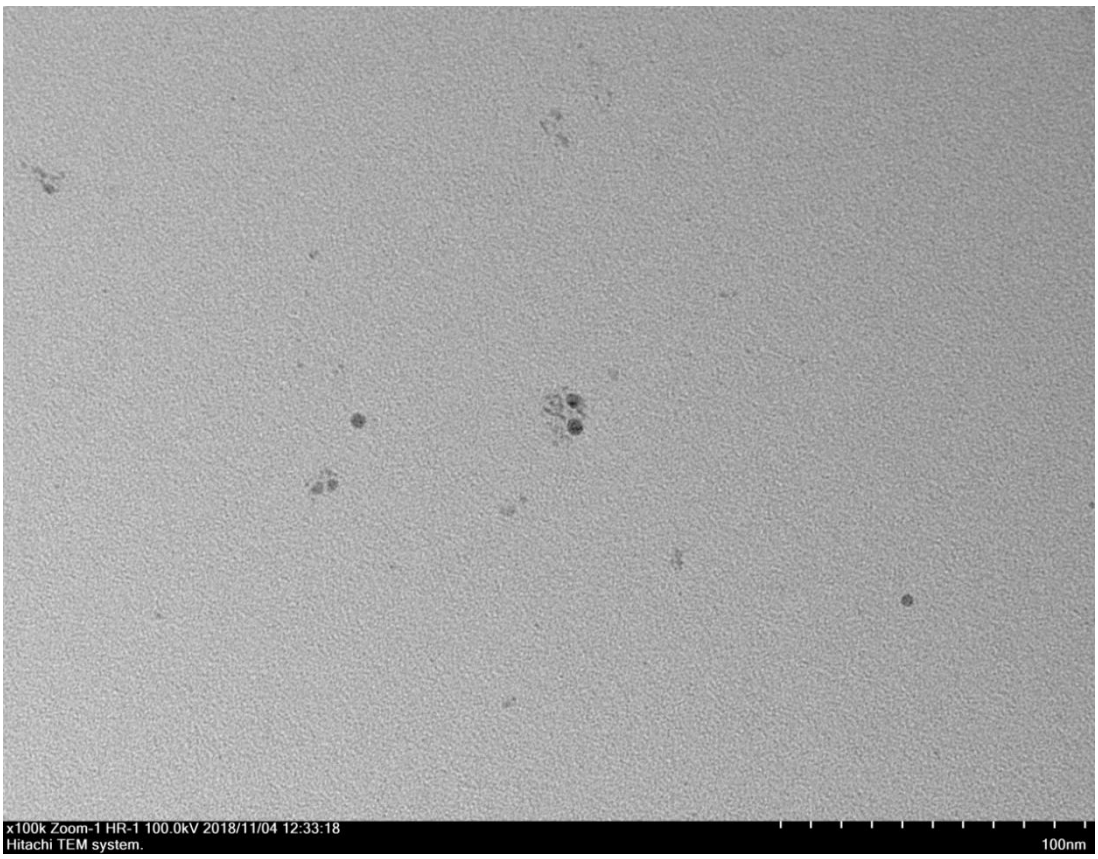

Figure S3. TEM image of palladium nanoparticles formed by Method A in the presence of Buchwald ligand. 100k magnification.

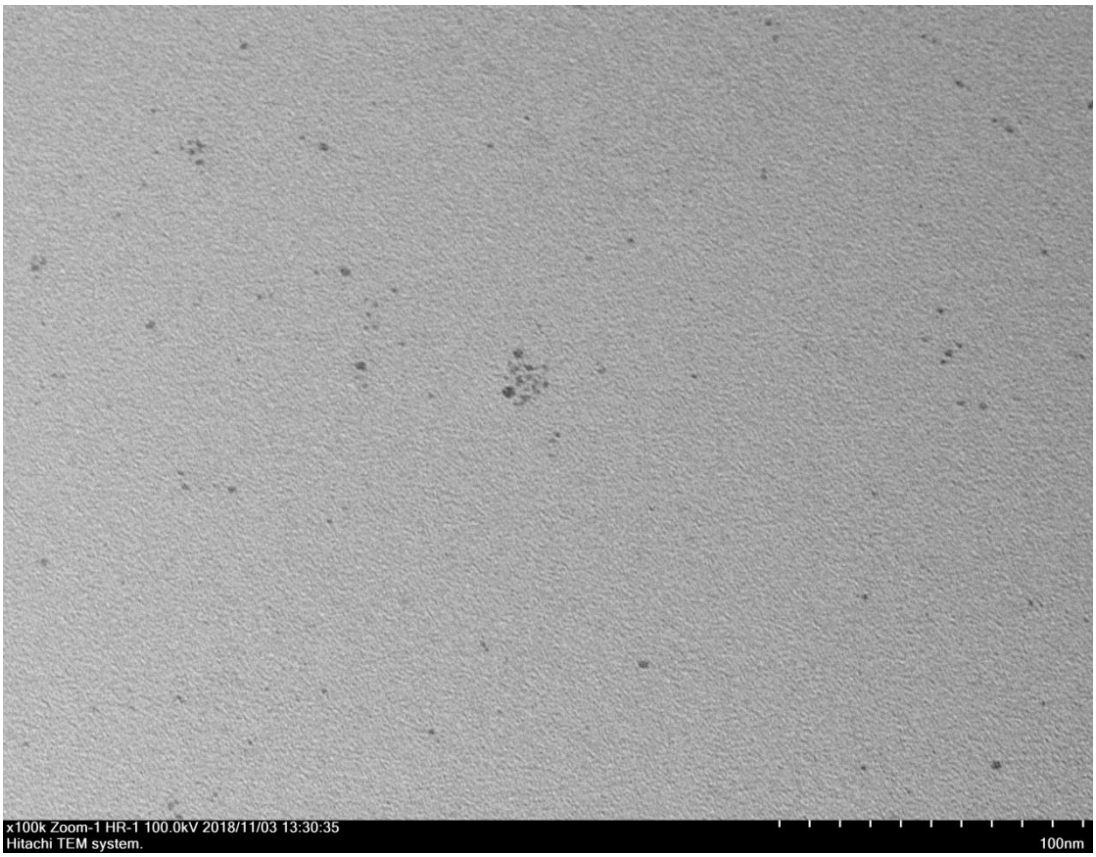

Figure S4. TEM image of palladium nanoparticles formed by Method A in the presence of BINAP. 100k magnification.

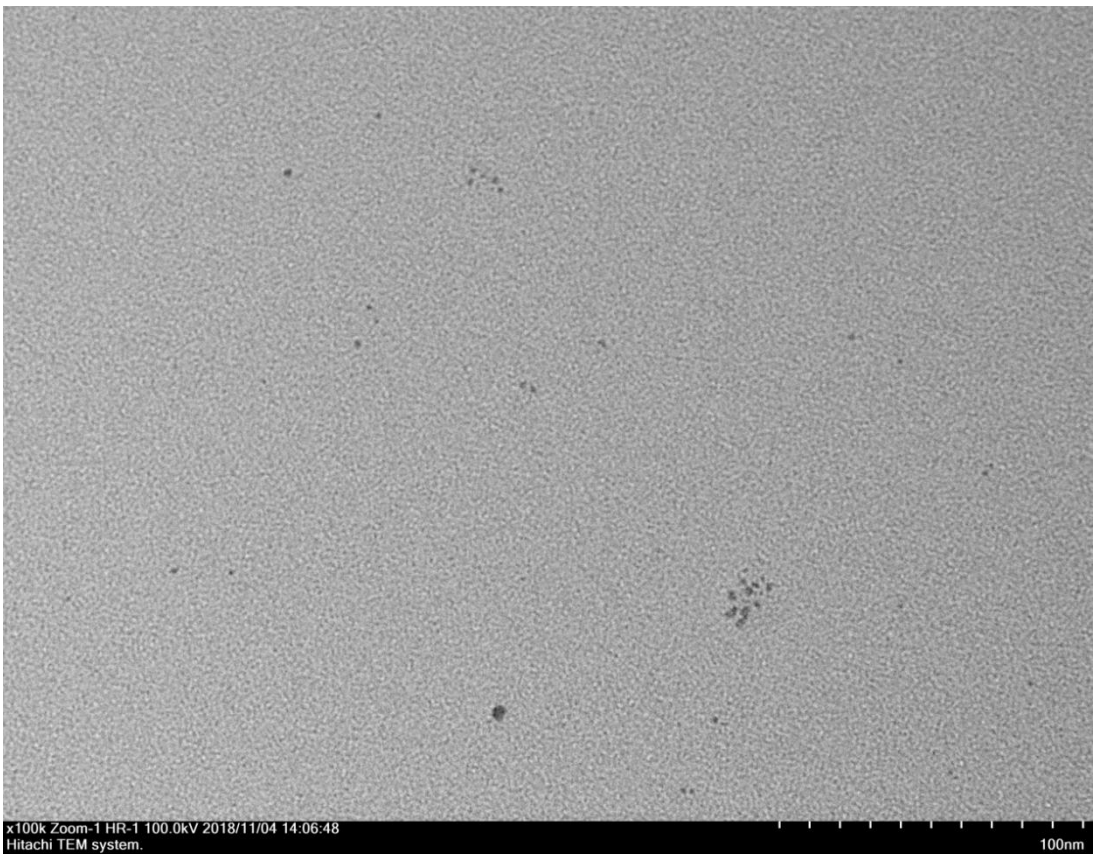

Figure S5. TEM image of palladium nanoparticles formed by Method A in the presence of triisopropyl phosphite. 100k magnification.

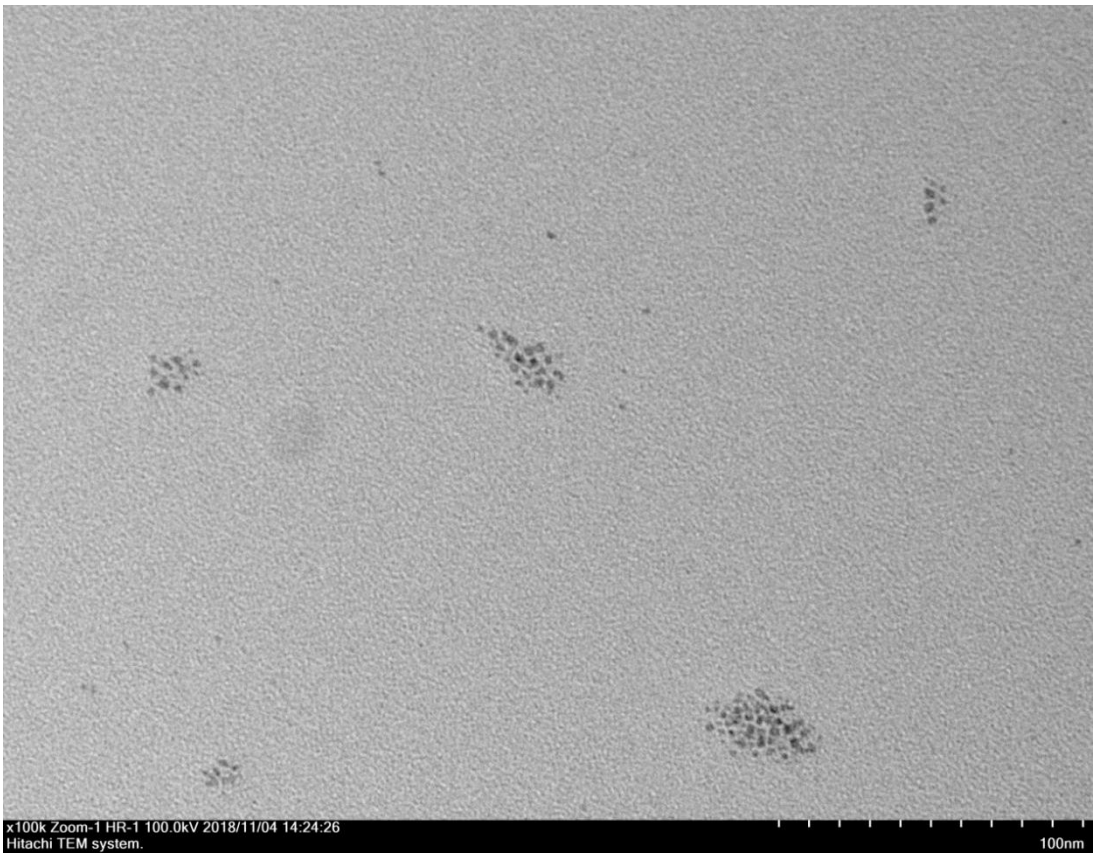

Figure S6. TEM image of palladium nanoparticles formed by Method A in the presence of tris-(4-chlorophenyl)phosphine. 100k magnification.

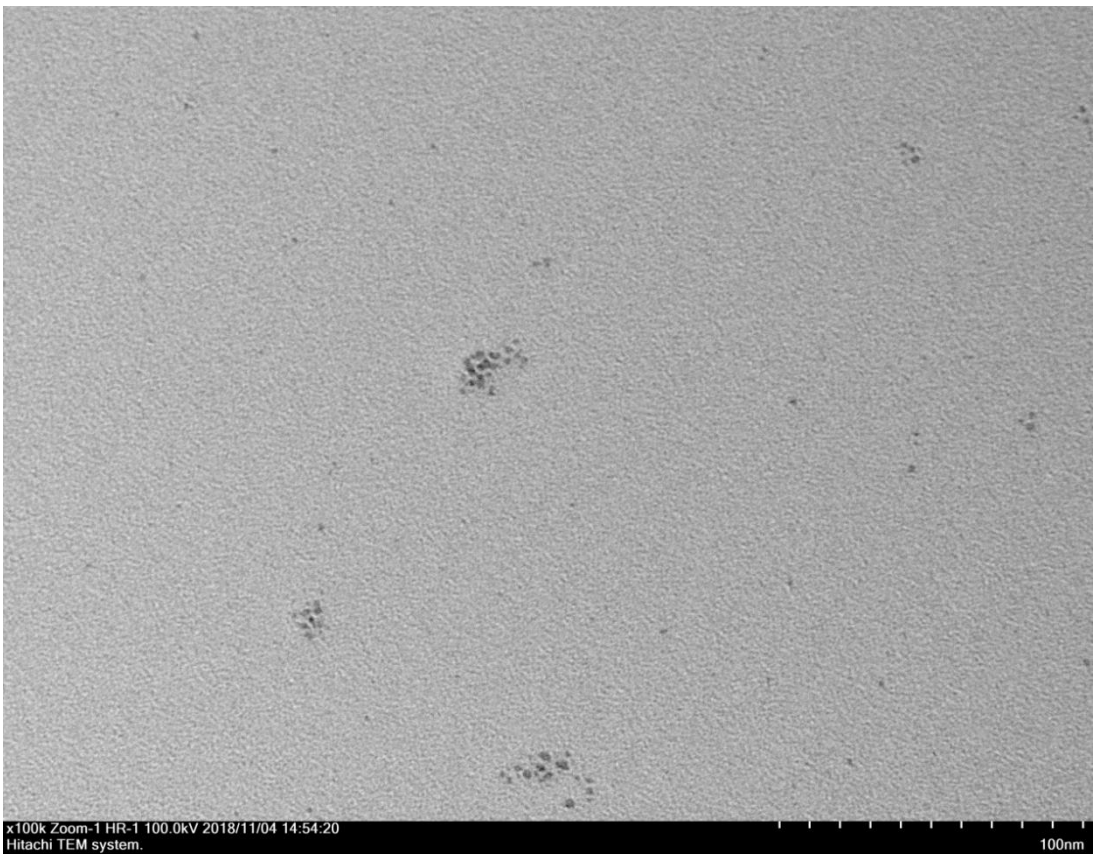

Figure S7. TEM image of palladium nanoparticles formed by Method A in the presence of DPPB. 100k magnification.

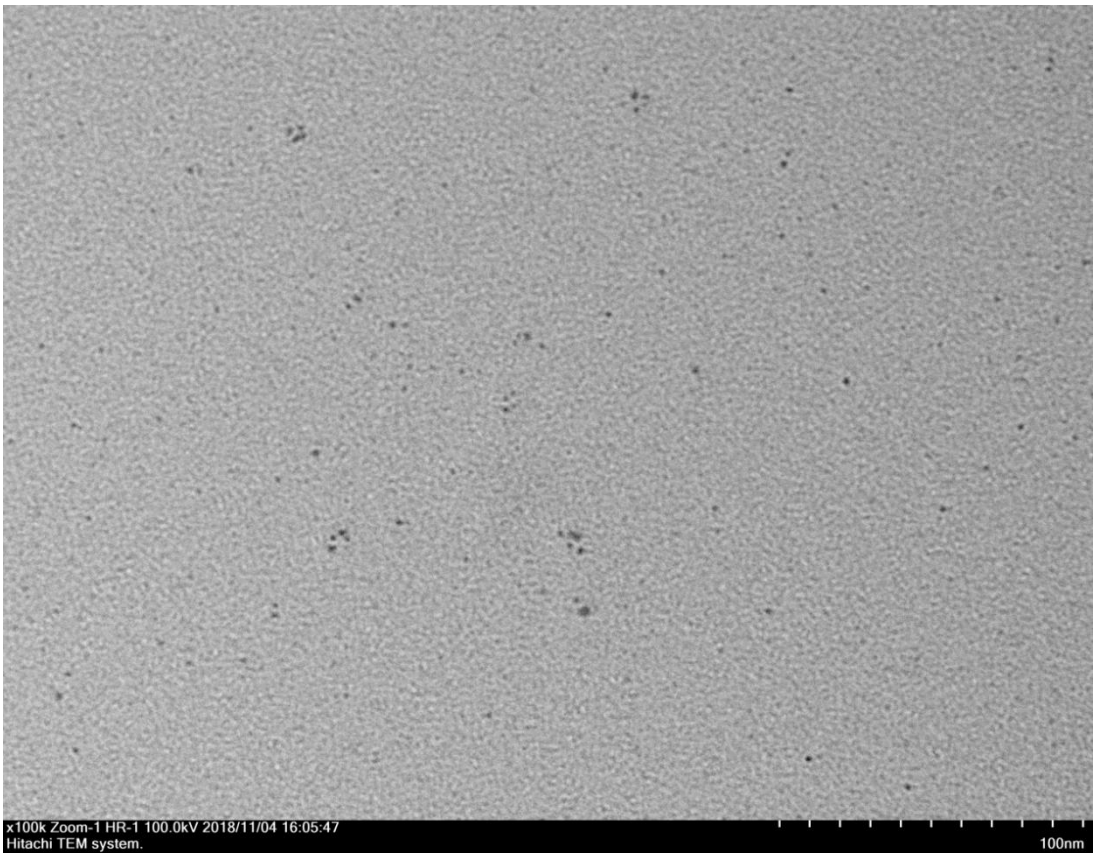

Figure S8. TEM image of palladium nanoparticles formed by Method A in the presence of DPPM. 100k magnification.

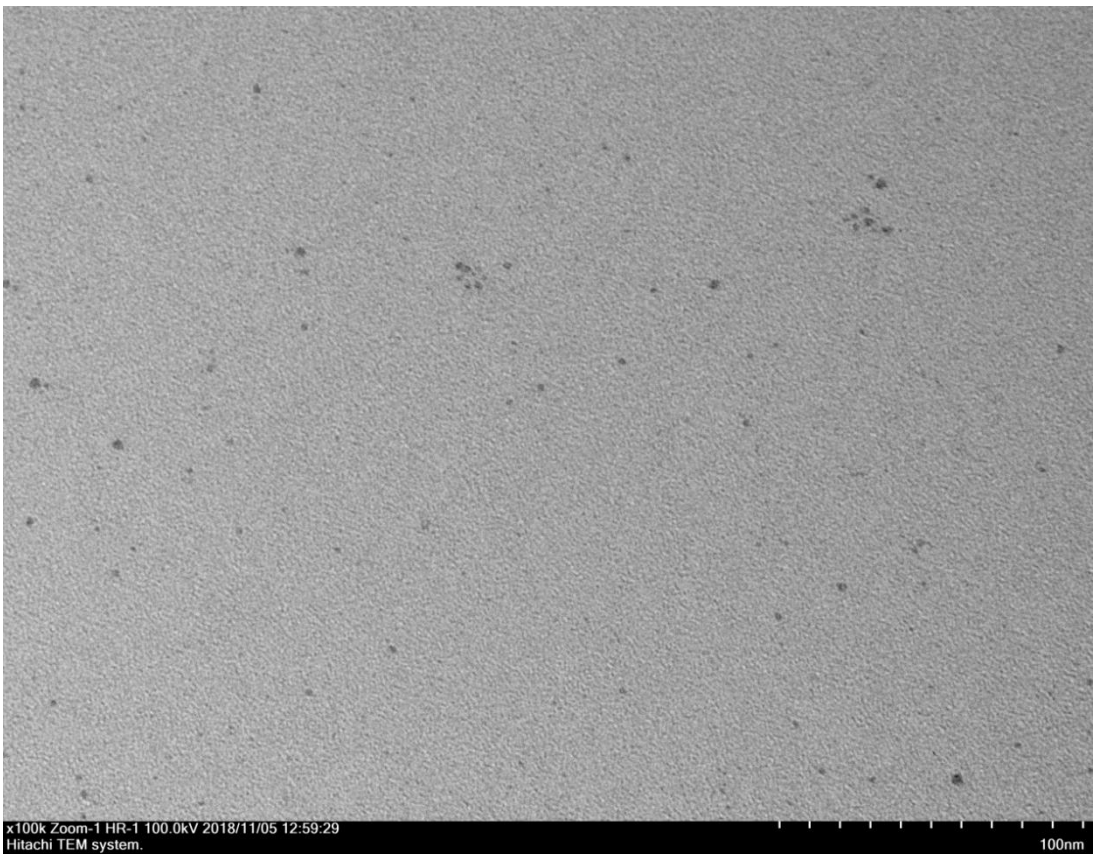

Figure S9. TEM image of palladium nanoparticles formed by Method A in the presence of DPPF. 100k magnification.

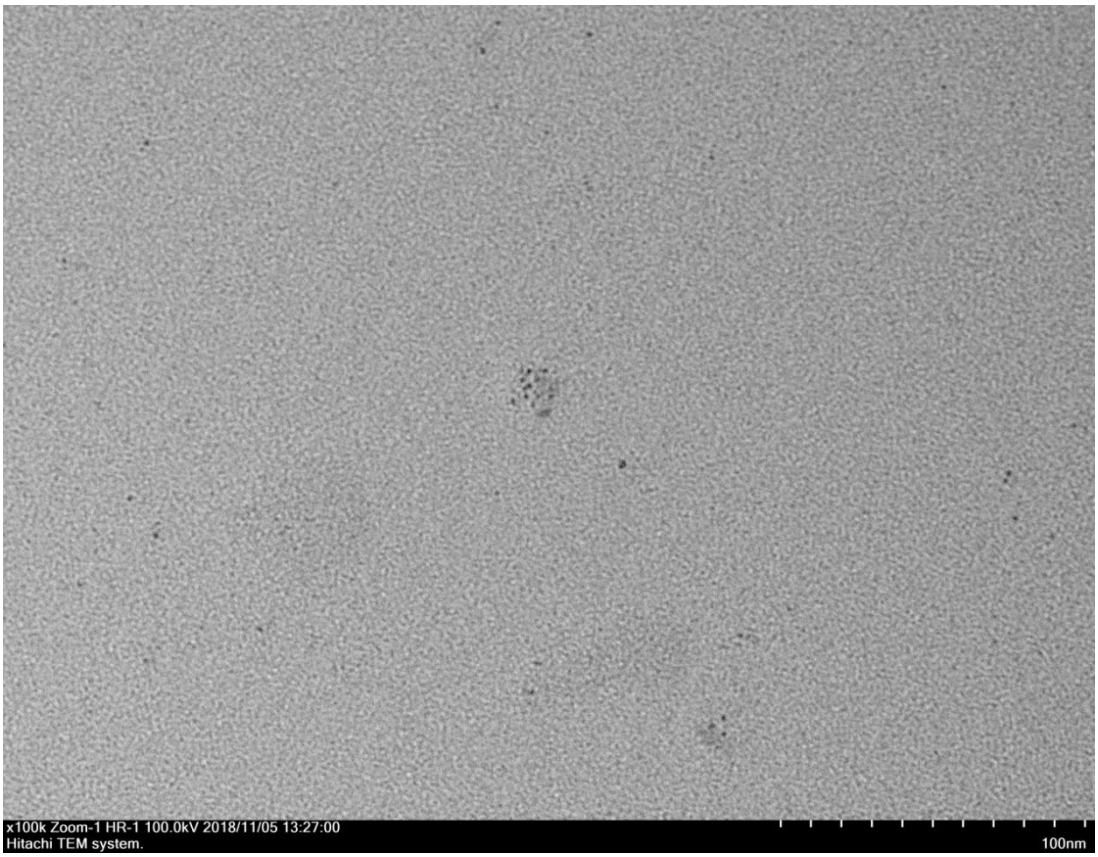

Figure S10. TEM image of palladium nanoparticles formed according by Method A in the presence of Xantphos. 100k magnification.

S5. Metallic nanoparticles formed in water solutions

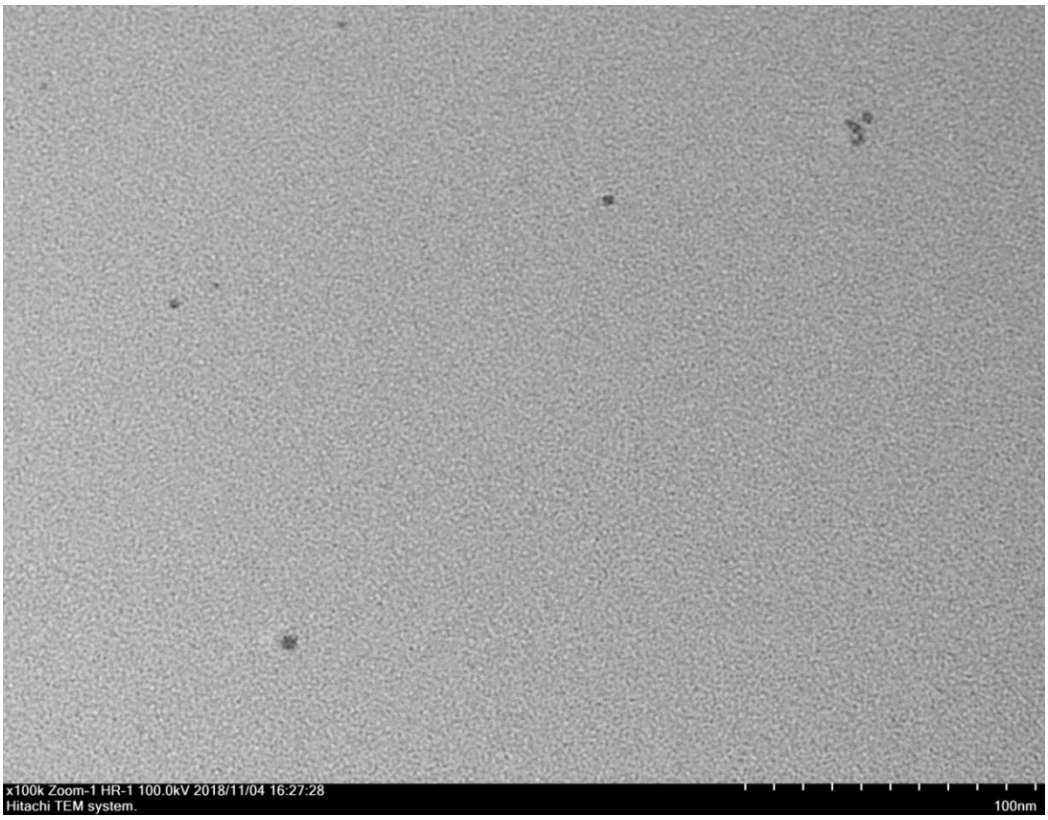

Figure S11. TEM image of copper nanoparticles formed by Method B. 100k magnification.

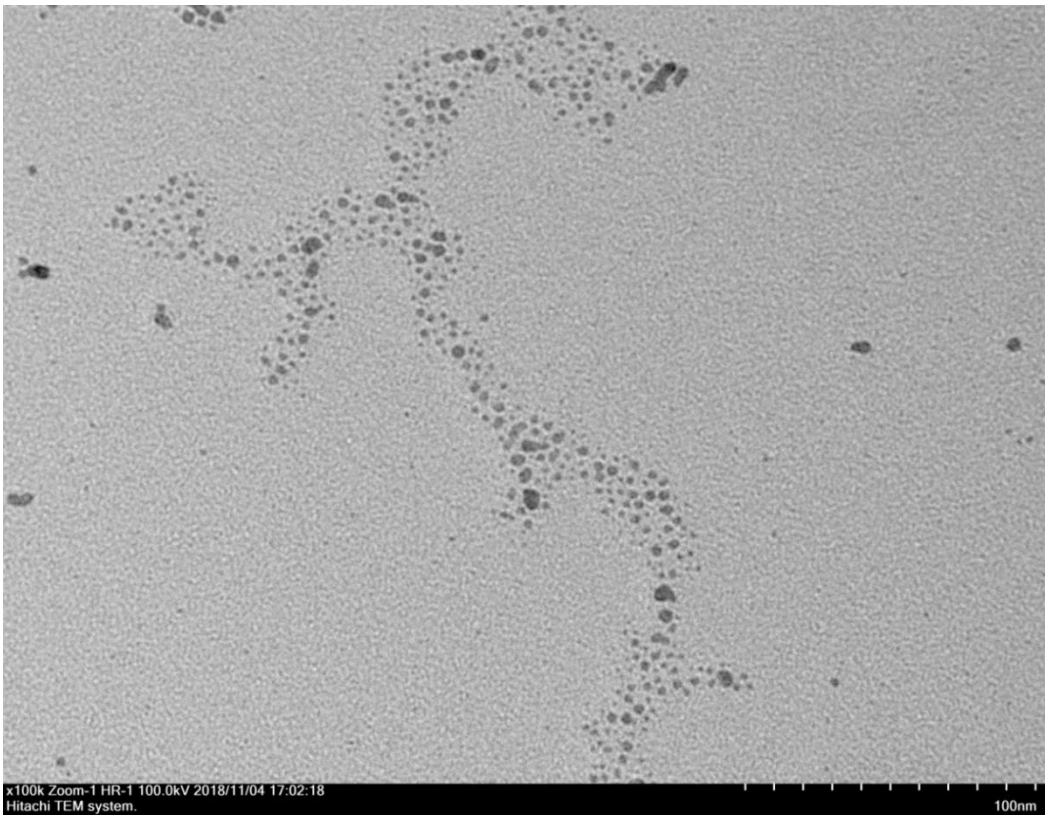

Figure S12. TEM image of palladium nanoparticles formed by Method B. 100k magnification.

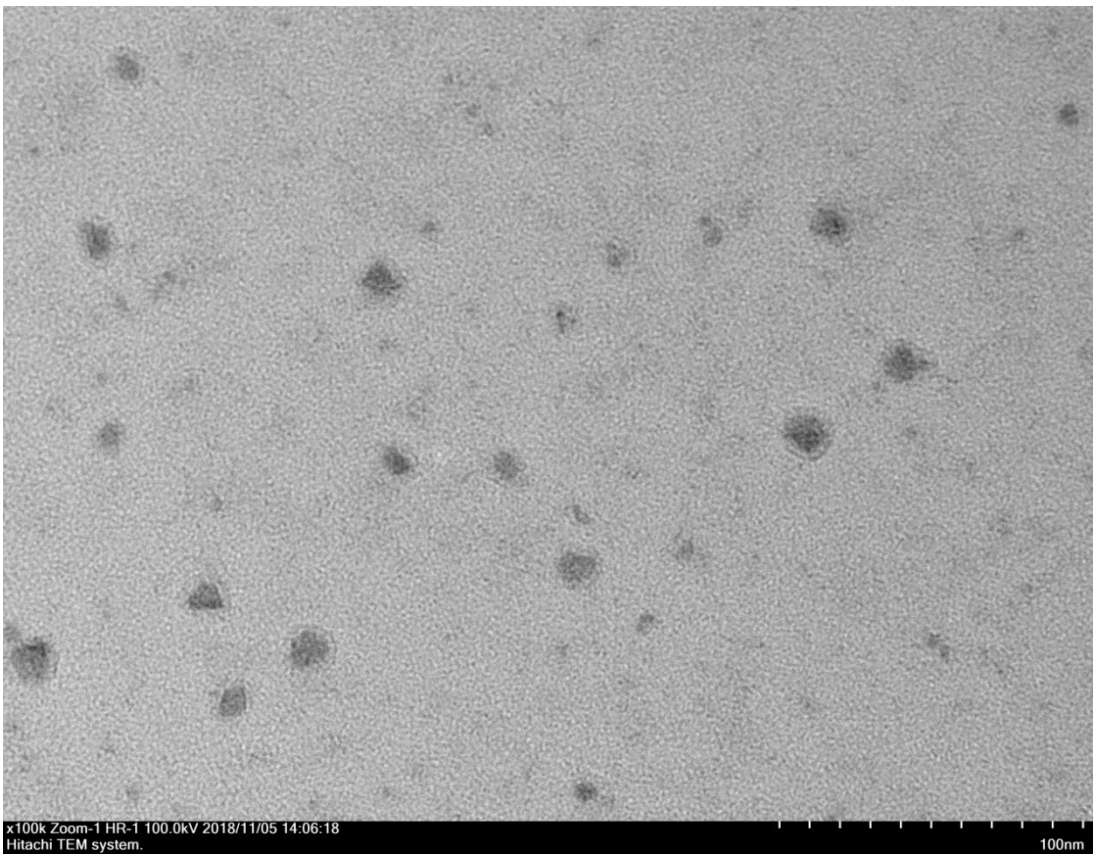

Figure S13. TEM image of nickel nanoparticles formed by Method B. 100k magnification.

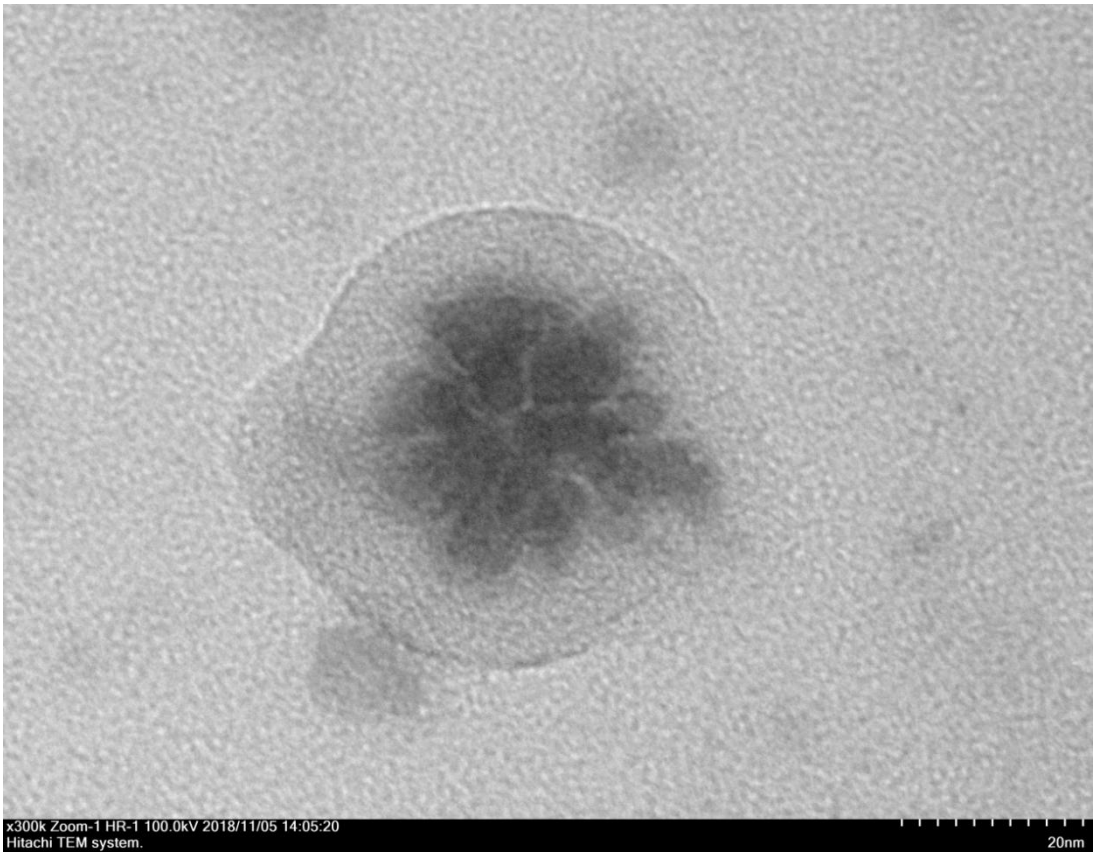

Figure S14. TEM image of nickel nanoparticles formed by Method B. 300k magnification.

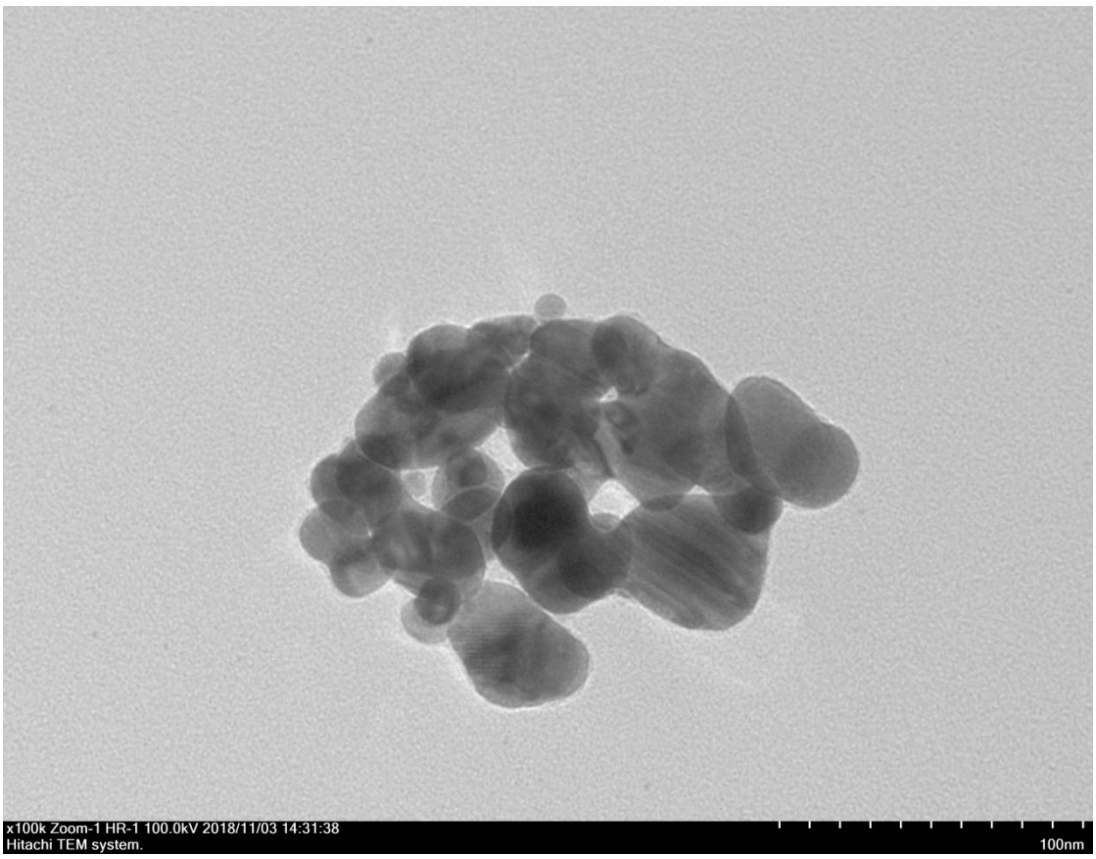

Figure S15. TEM image of silver nanoparticles formed by Method B. 100k magnification.

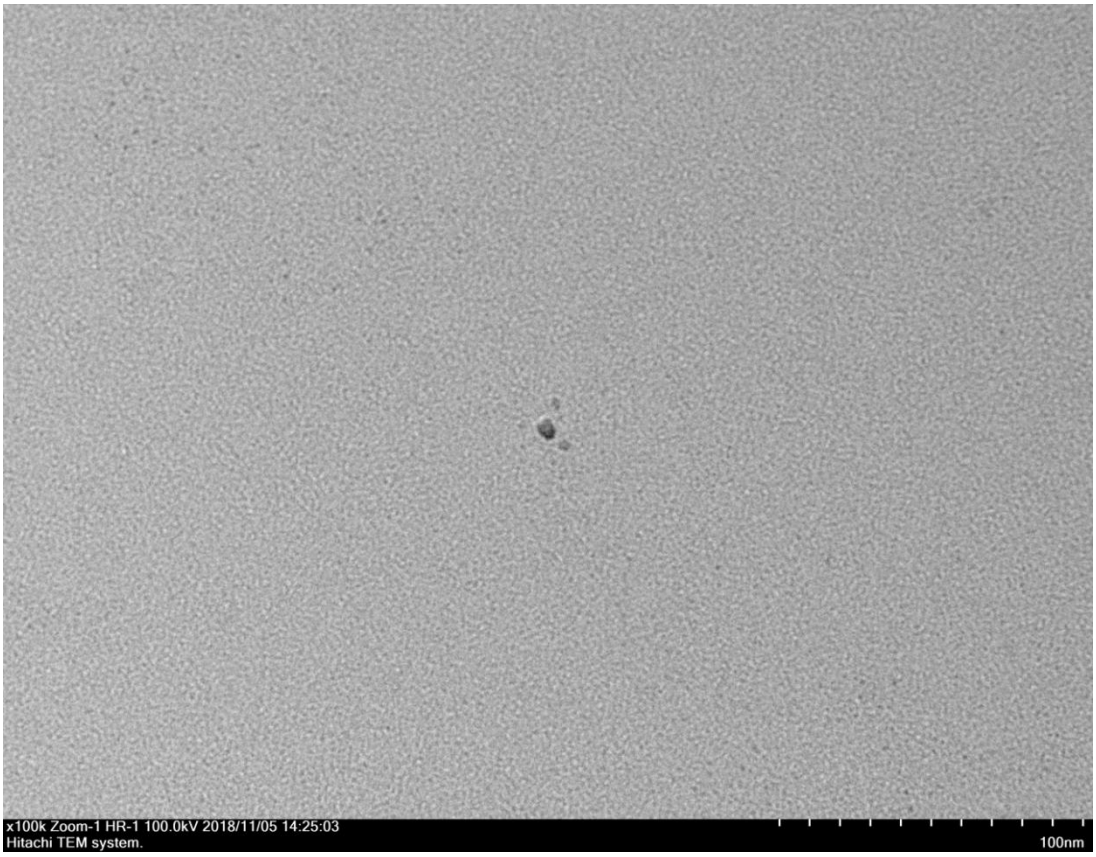

Figure S16. TEM image of cobalt nanoparticles formed by Method B. 100k magnification.

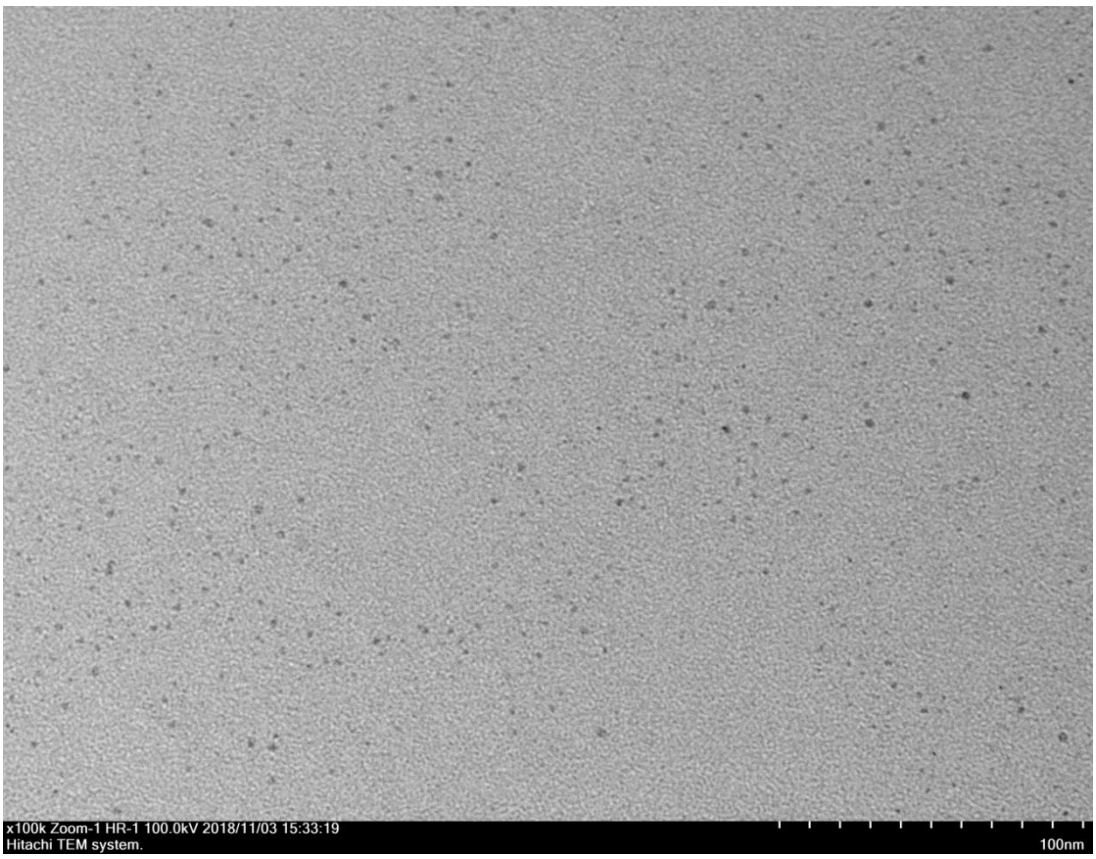

Figure S17. TEM image of rhodium nanoparticles formed by Method B. 100k magnification.

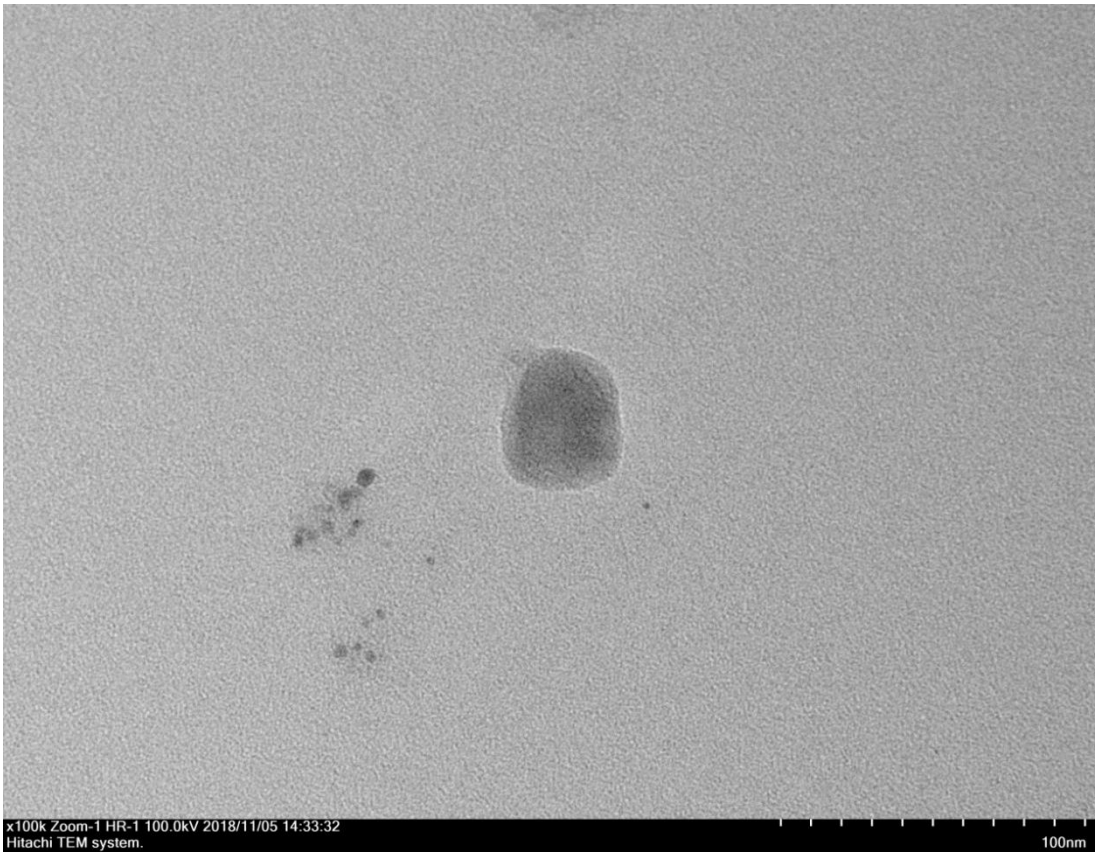

Figure S18. TEM image of chromium nanoparticles formed by Method B. 100k magnification.

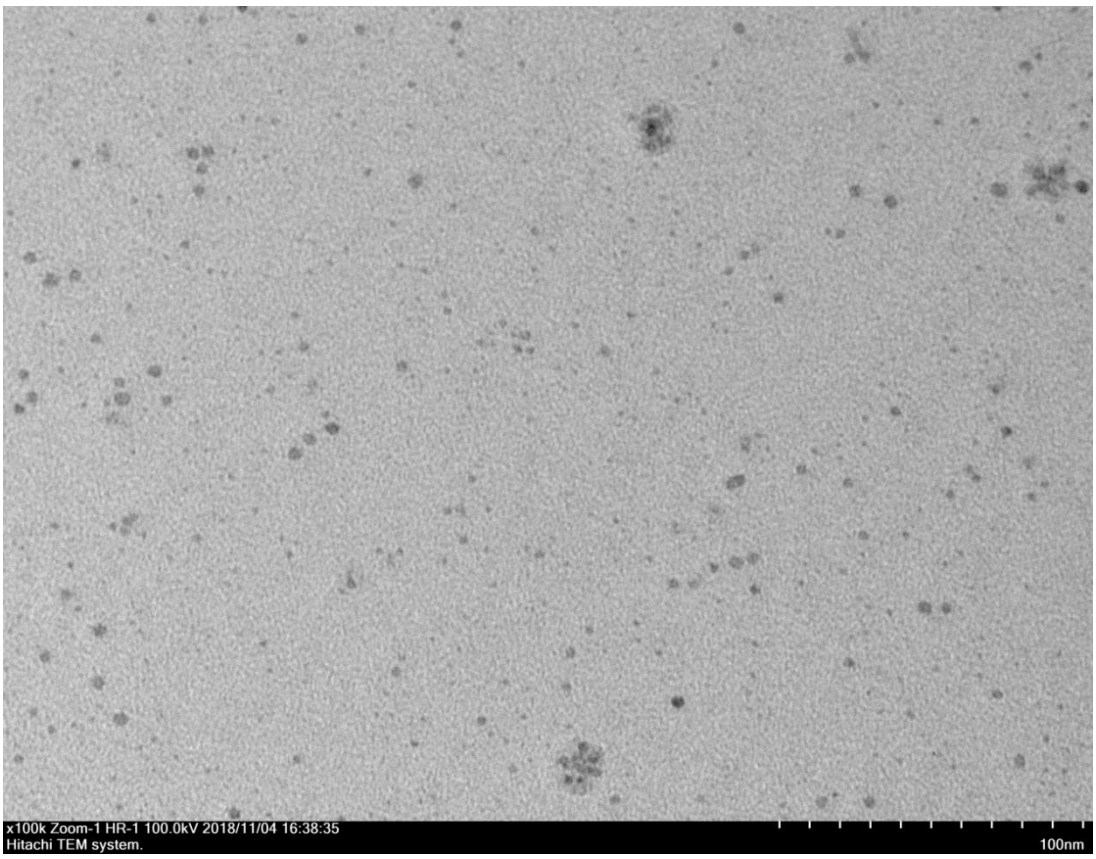

Figure S19. TEM image of cadmium nanoparticles formed by Method B. 100k magnification.

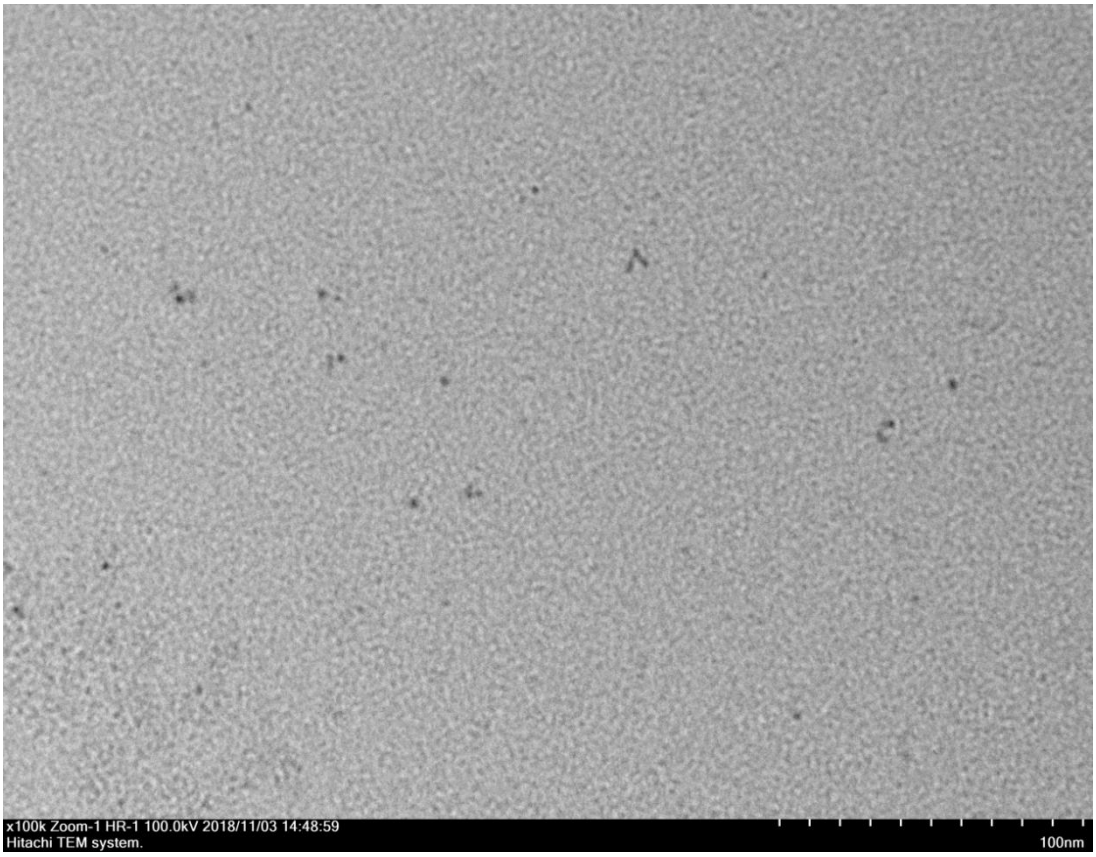

Figure S20. TEM image of iridium nanoparticles formed by Method B. 100k magnification.

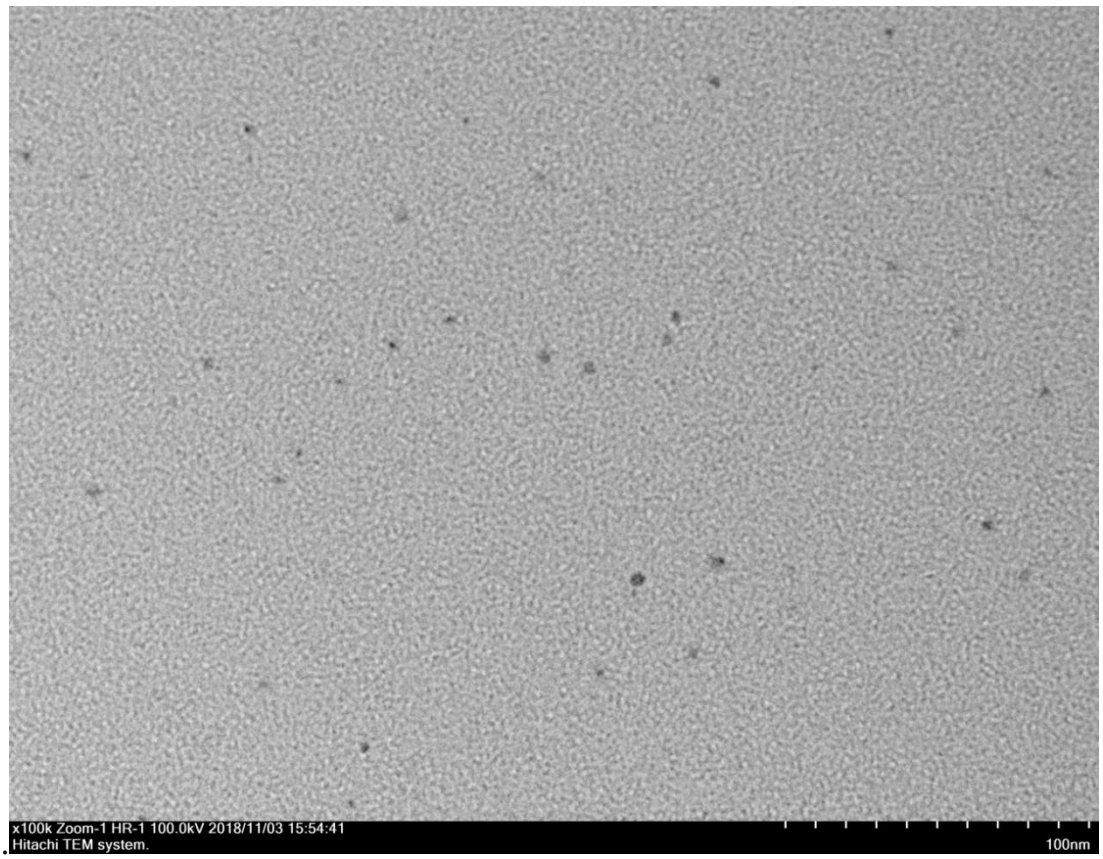

Figure S21. TEM image of ruthenium nanoparticles formed by Method B. 100k magnification.

S6. Palladium nanoparticles found in the Heck reaction mixture

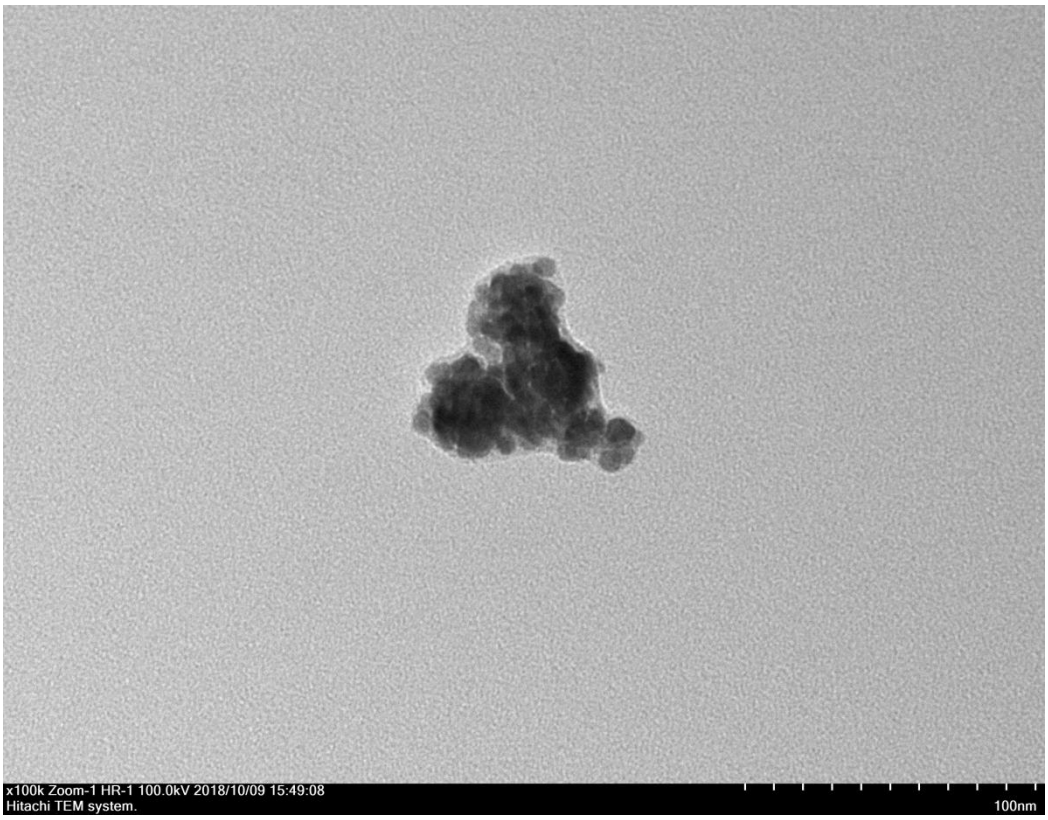

Figure S22. TEM image of palladium nanoparticles obtained at 0.5 h of Heck reaction with heterogeneous catalyst precursor. 100k magnification.

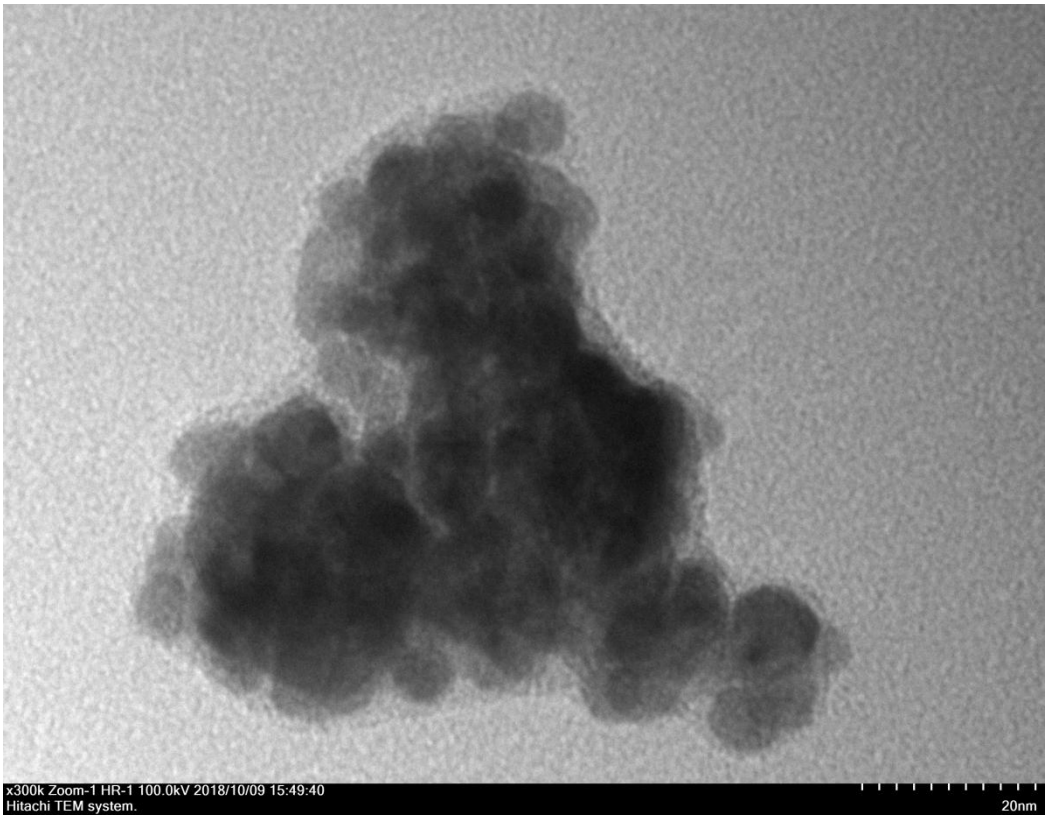

Figure S23. TEM image of palladium nanoparticles obtained at 0.5 h of Heck reaction with heterogeneous catalyst precursor. 300k magnification.

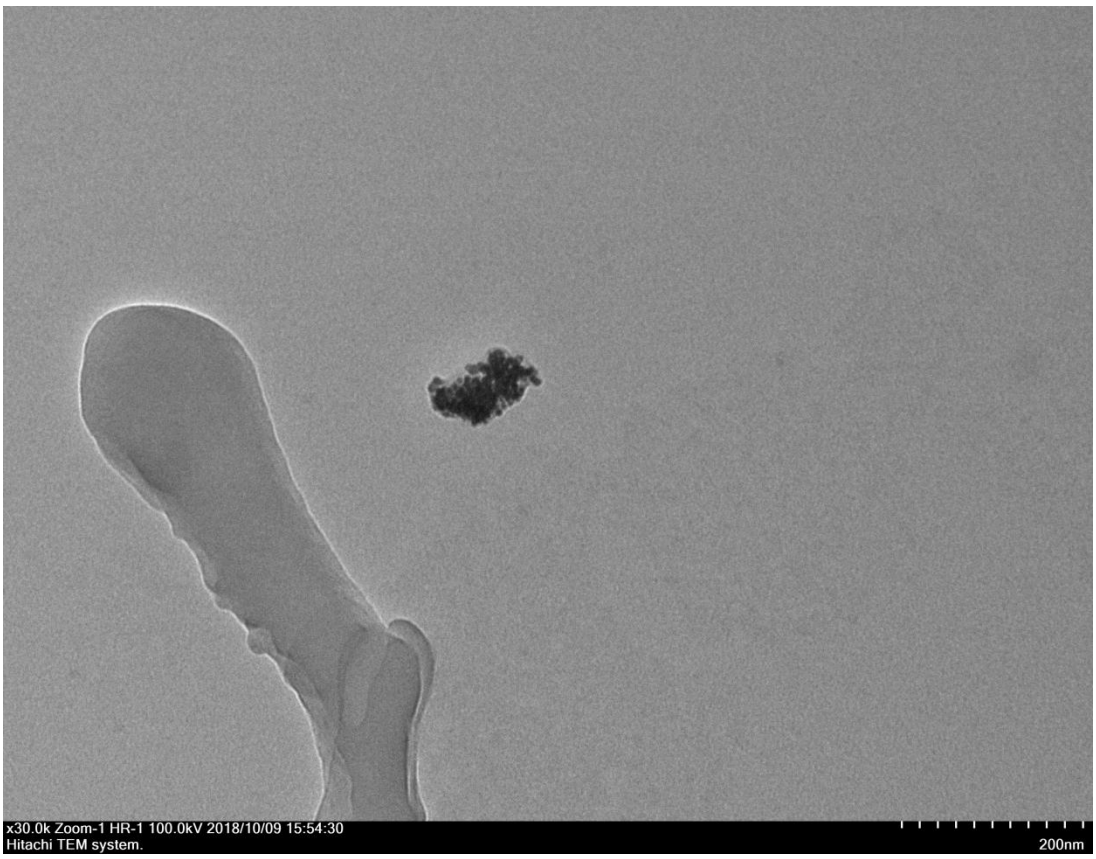

Figure S24. TEM image of palladium nanoparticles obtained at 0.5 h of Heck reaction with heterogeneous catalyst precursor. 30k magnification.

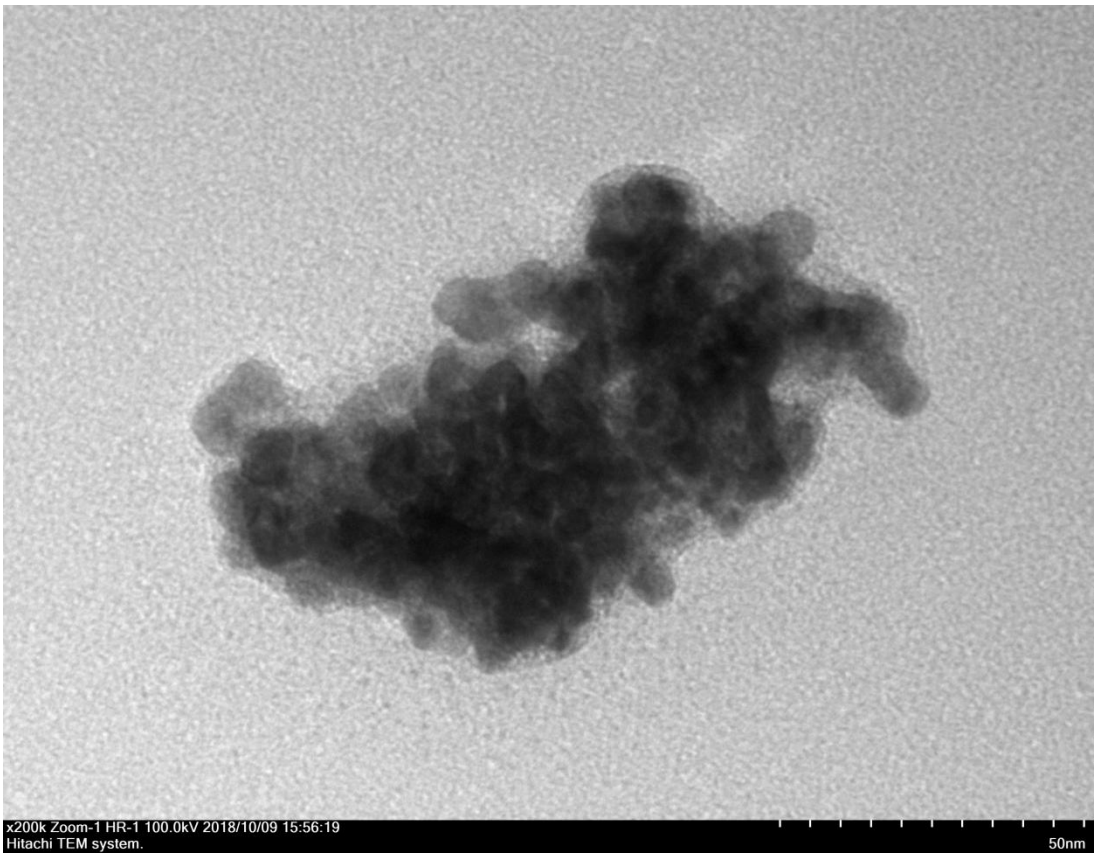

Figure S25. TEM image of palladium nanoparticles obtained at 0.5 h of Heck reaction with heterogeneous catalyst precursor. 200k magnification.

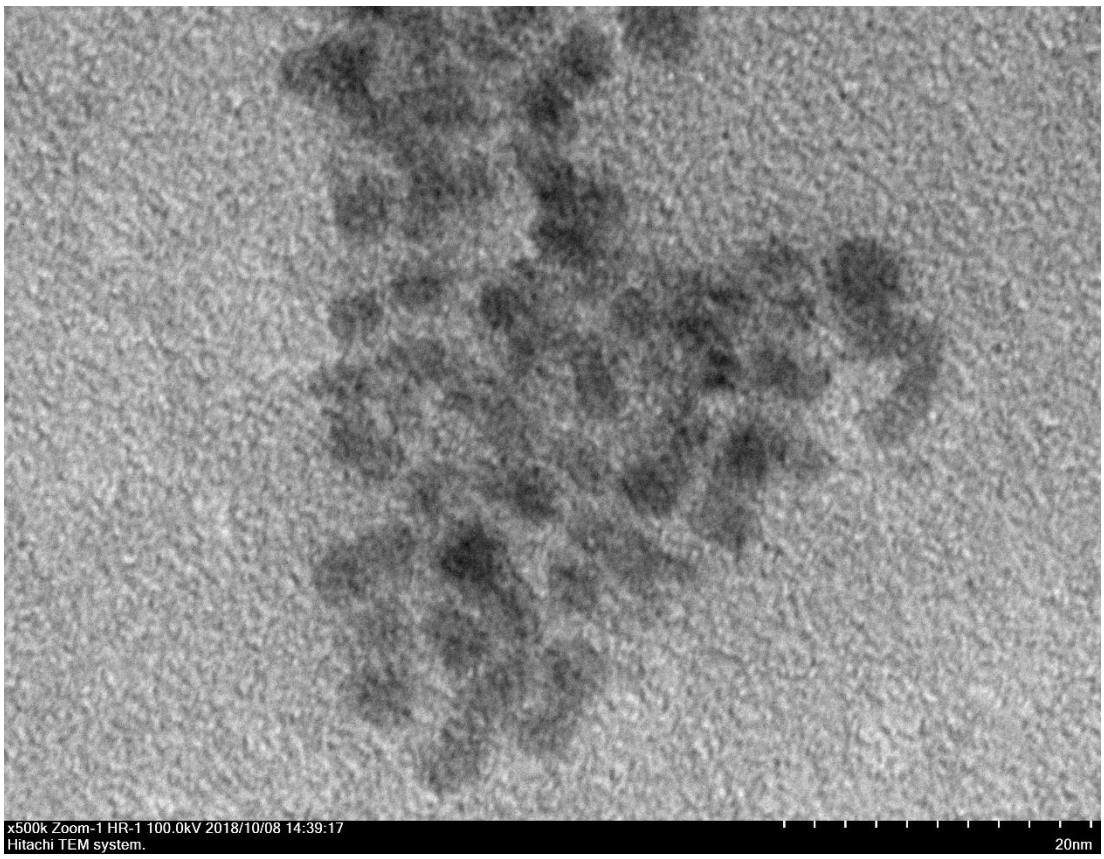

Figure S26. TEM image of palladium nanoparticles obtained at 0.5 h of Heck reaction with heterogeneous catalyst precursor. 500k magnification.

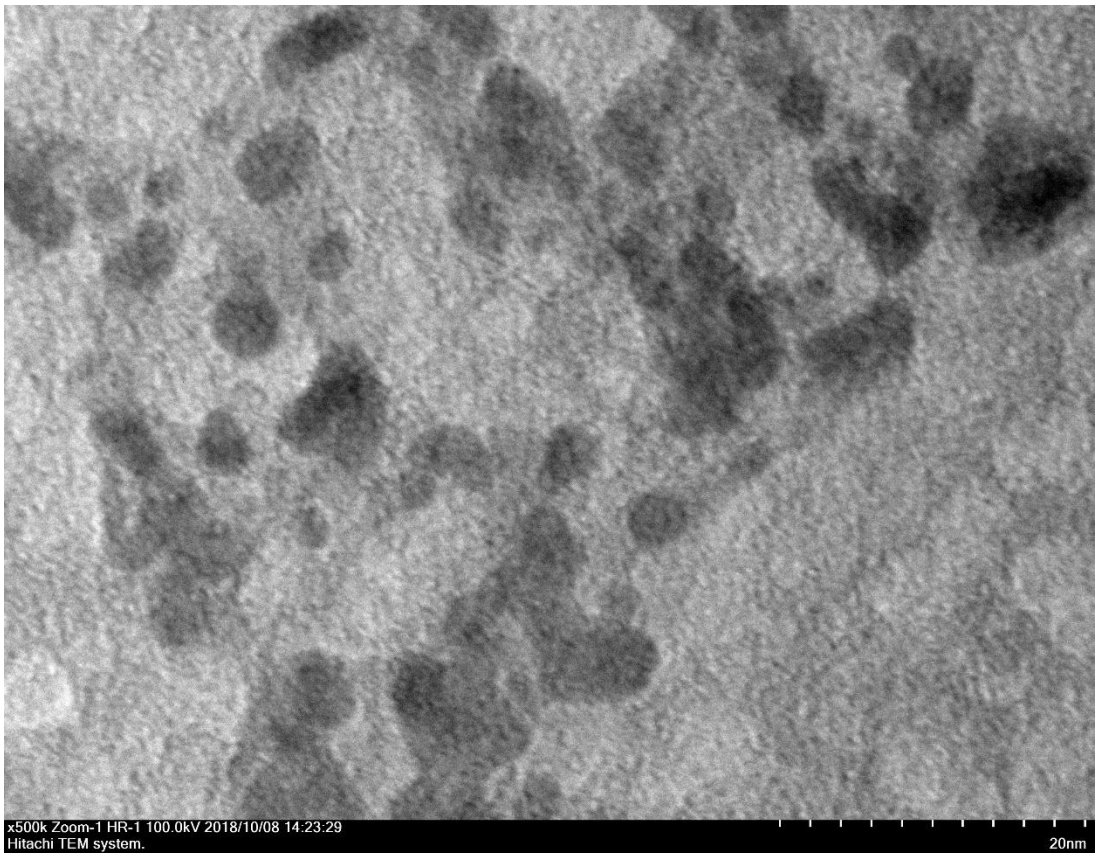

Figure S27. TEM image of palladium nanoparticles obtained at 0.5 h of Heck reaction with heterogeneous catalyst precursor. 500k magnification.

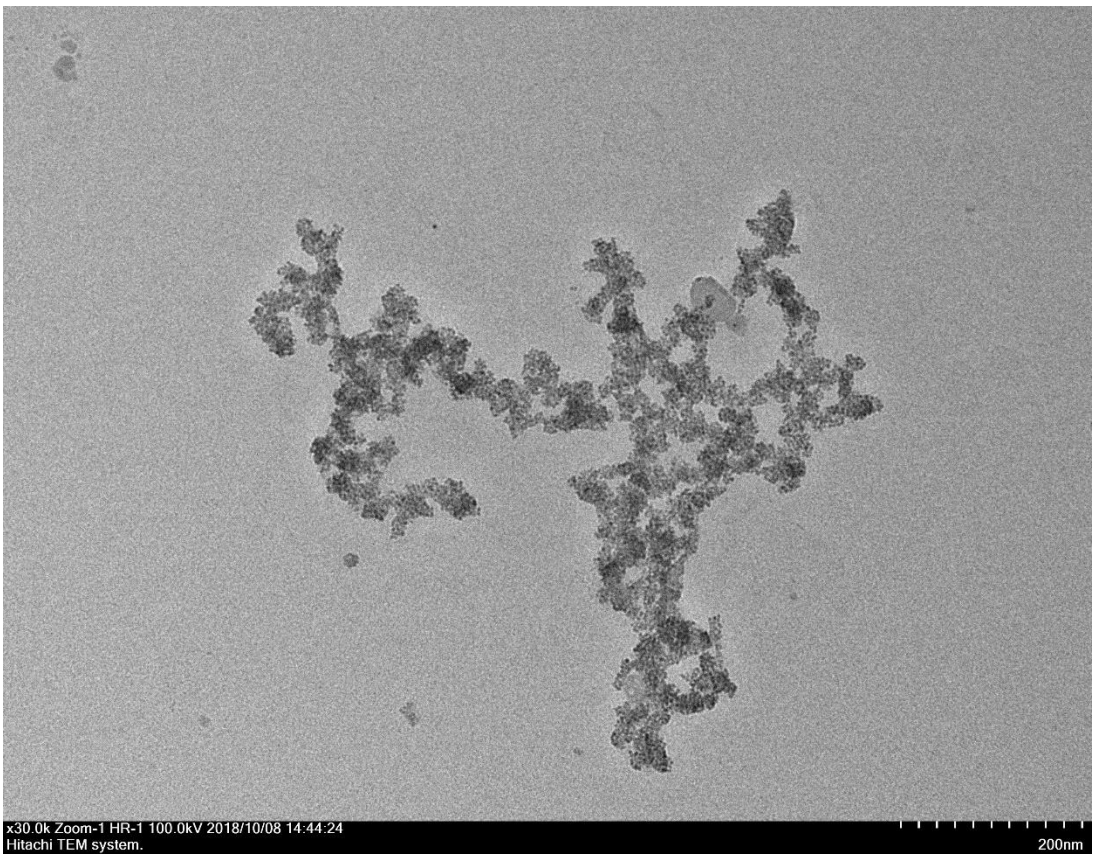

Figure S28. TEM image of palladium nanoparticles obtained at 0.5 h of Heck reaction with heterogeneous catalyst precursor. 30k magnification.

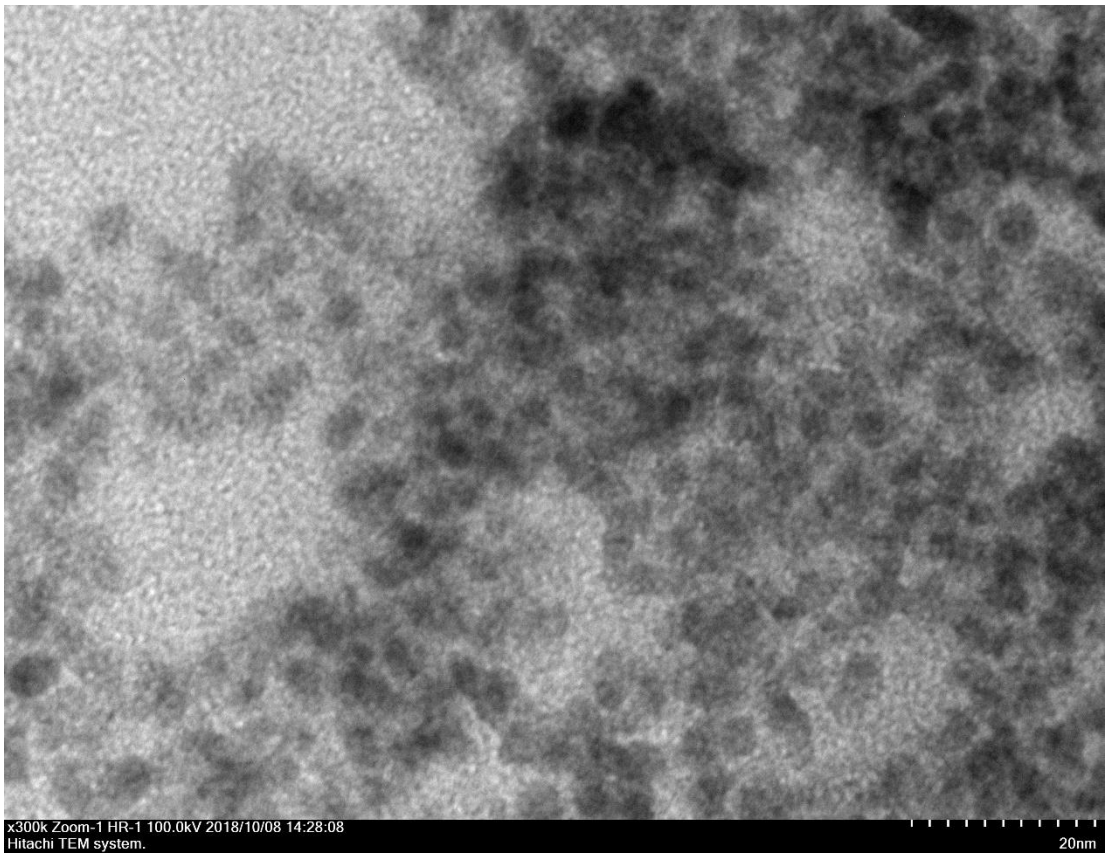

Figure S29. TEM image of palladium nanoparticles obtained at 0.5 h of Heck reaction with heterogeneous catalyst precursor. 300k magnification.

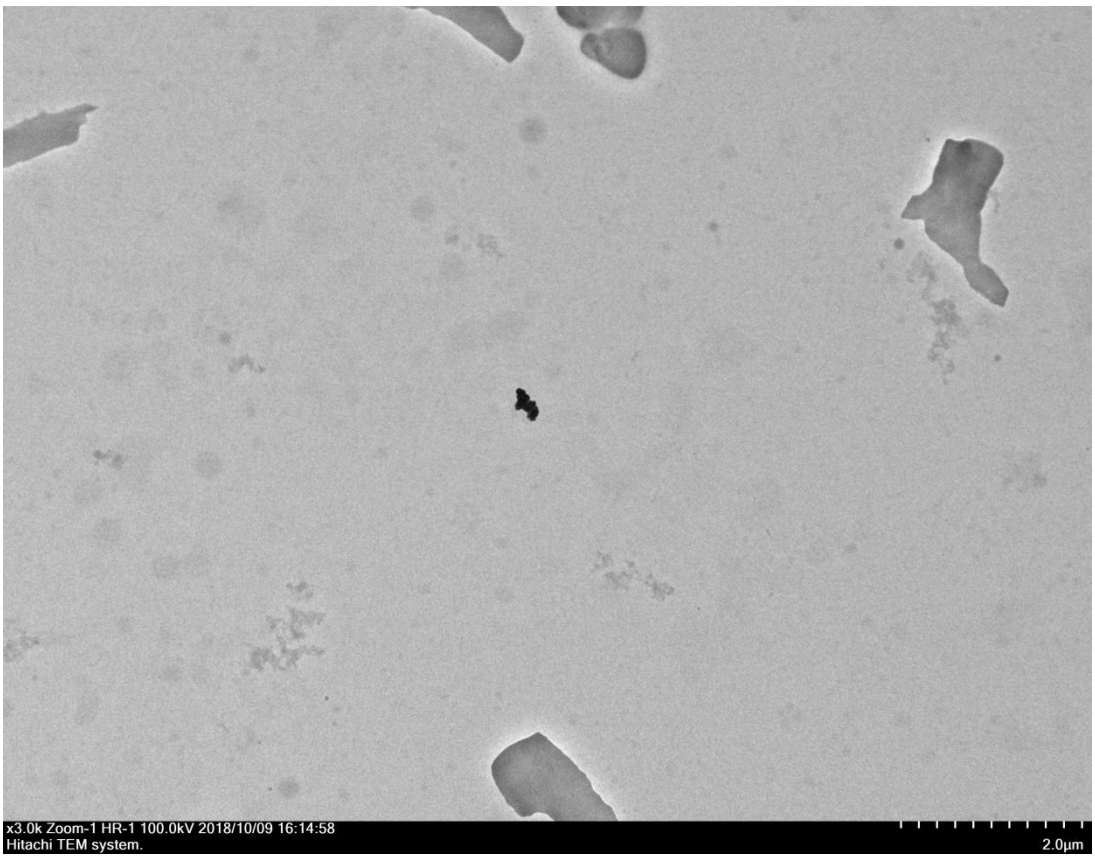

Figure S30. TEM image of palladium nanoparticles obtained at 1.0 h of Heck reaction with heterogeneous catalyst precursor. 3k magnification.

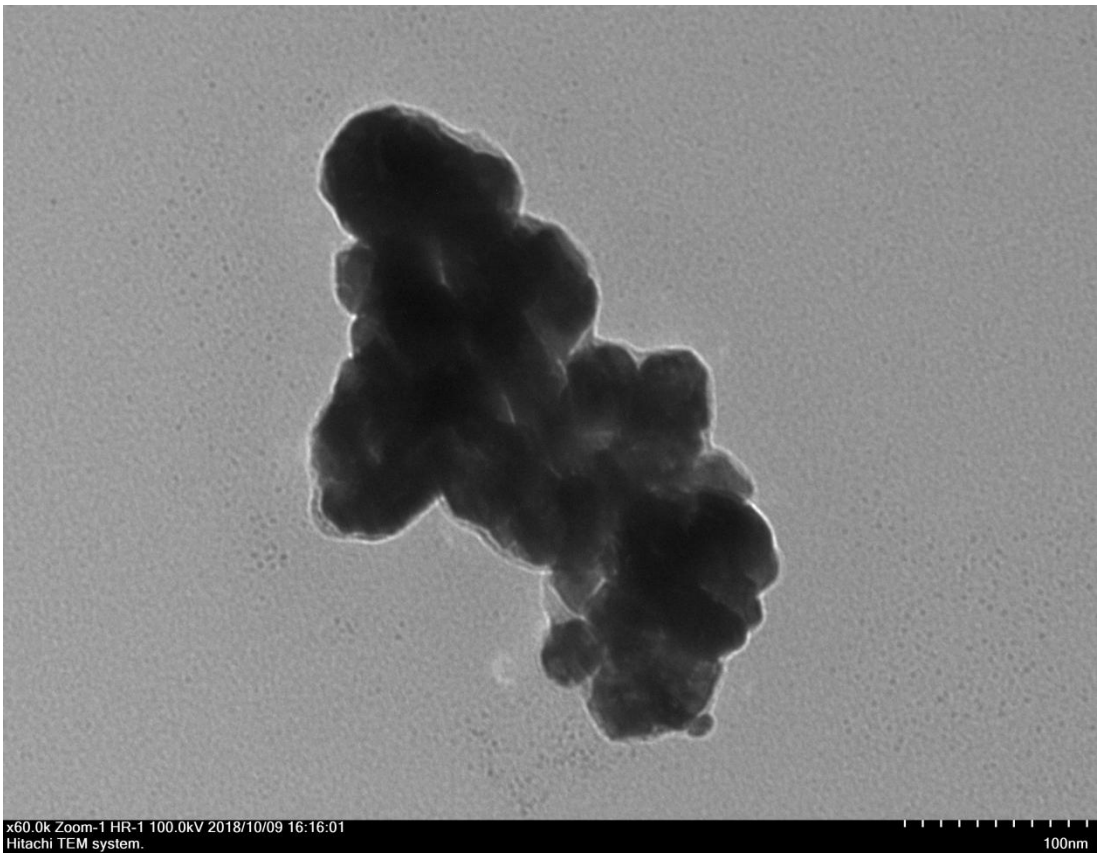

Figure S31. TEM image of palladium nanoparticles obtained at 1.0 h of Heck reaction with heterogeneous catalyst precursor. 60k magnification.

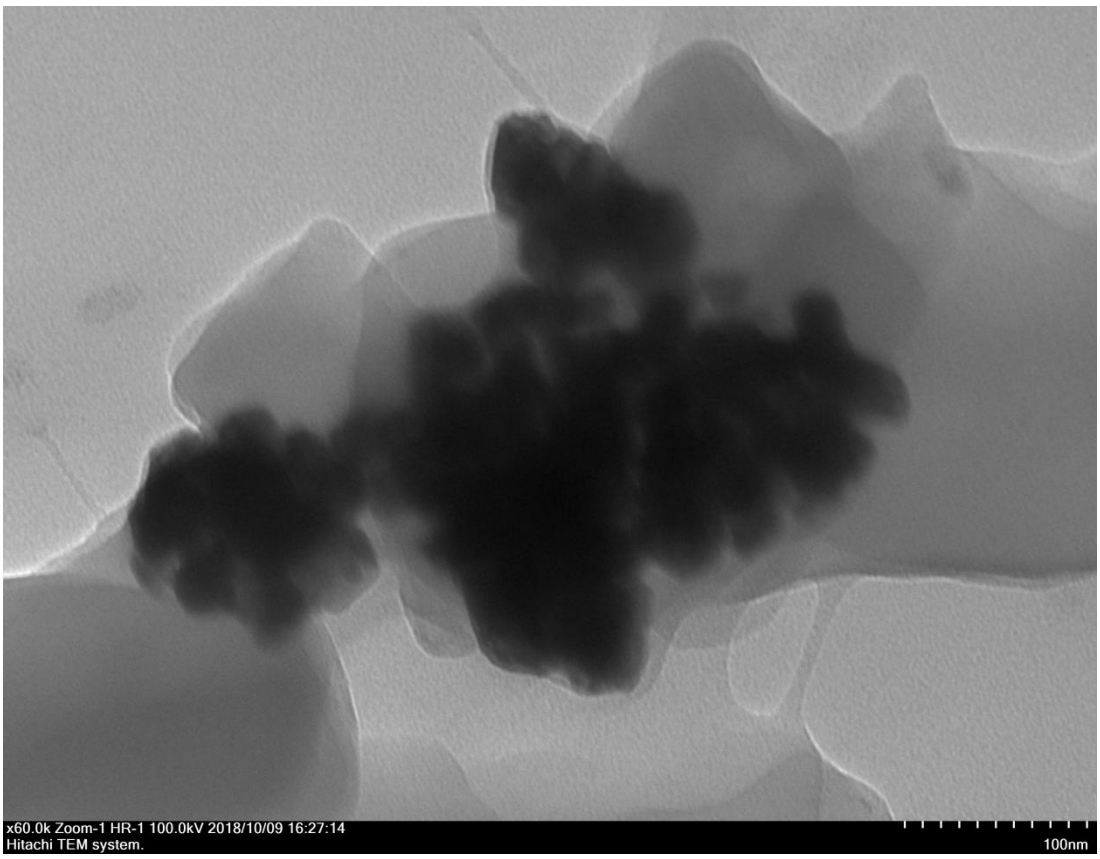

Figure S32. TEM image of palladium nanoparticles obtained at 1.0 h of Heck reaction with heterogeneous catalyst precursor. 60k magnification.

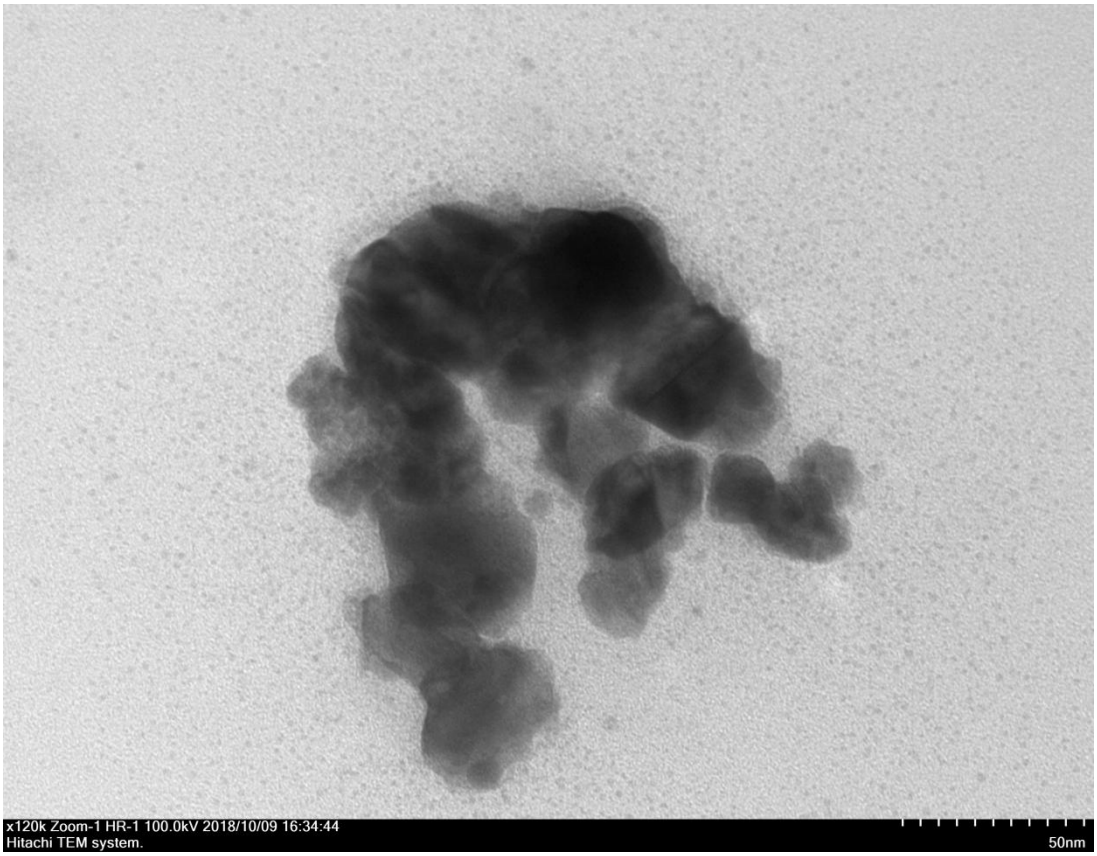

Figure S33. TEM image of palladium nanoparticles obtained at 1.0 h of Heck reaction with heterogeneous catalyst precursor. 120k magnification.

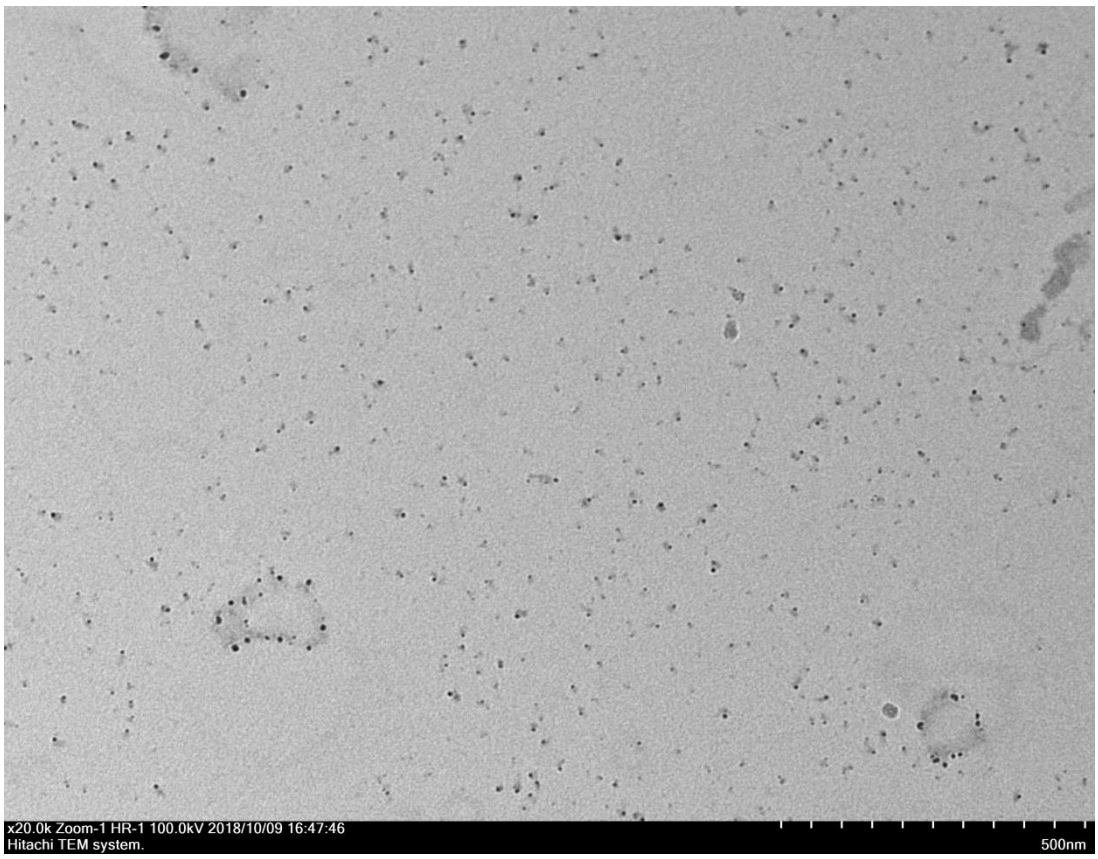

Figure S34. TEM image of palladium nanoparticles obtained at 2.0 h of Heck reaction with heterogeneous catalyst precursor. 20k magnification.

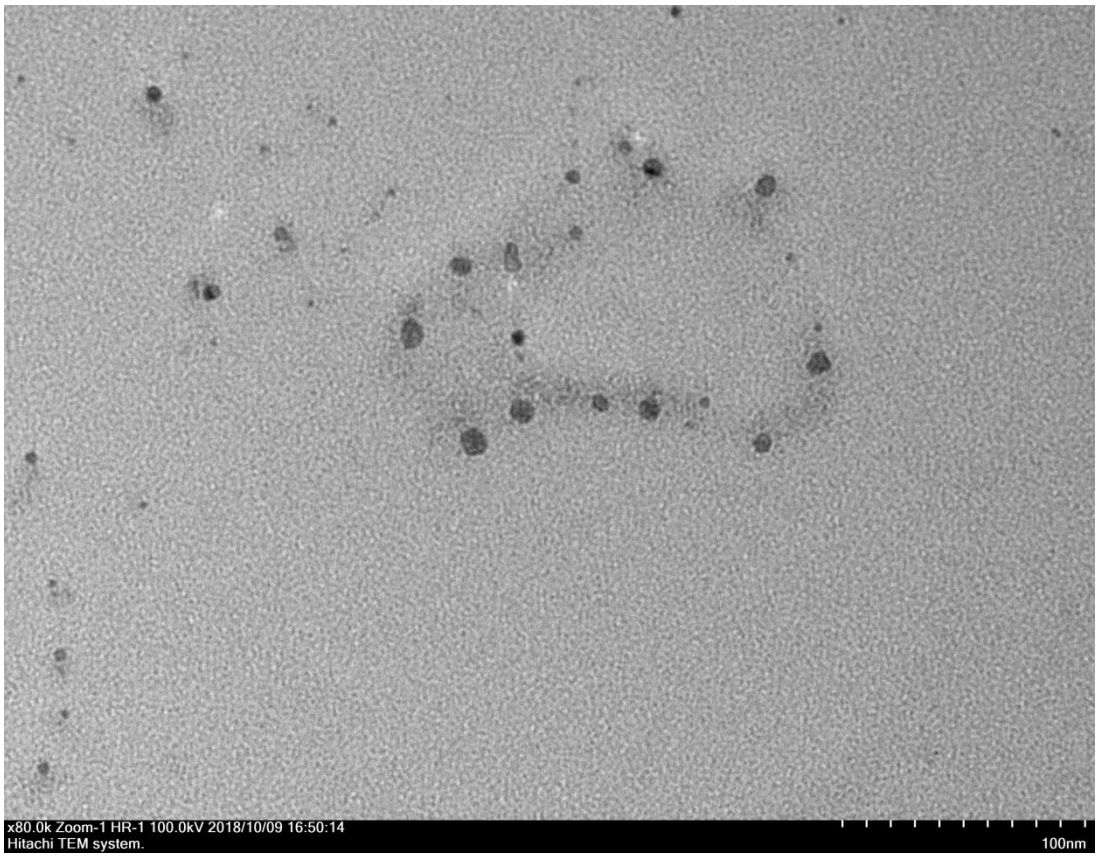

Figure S35. TEM image of palladium nanoparticles obtained at 2.0 h of Heck reaction with heterogeneous catalyst precursor. 80k magnification.

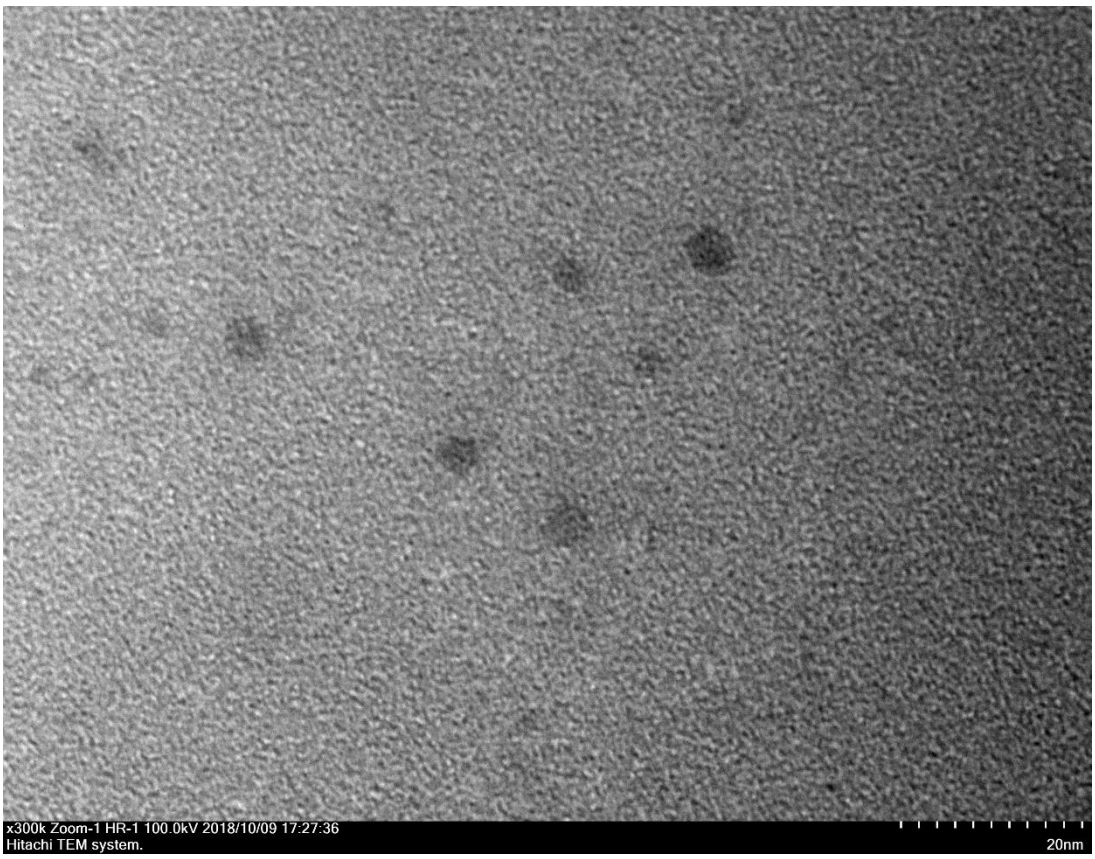

Figure S36. TEM image of palladium nanoparticles obtained at 2.0 h of Heck reaction with heterogeneous catalyst precursor. 300k magnification.

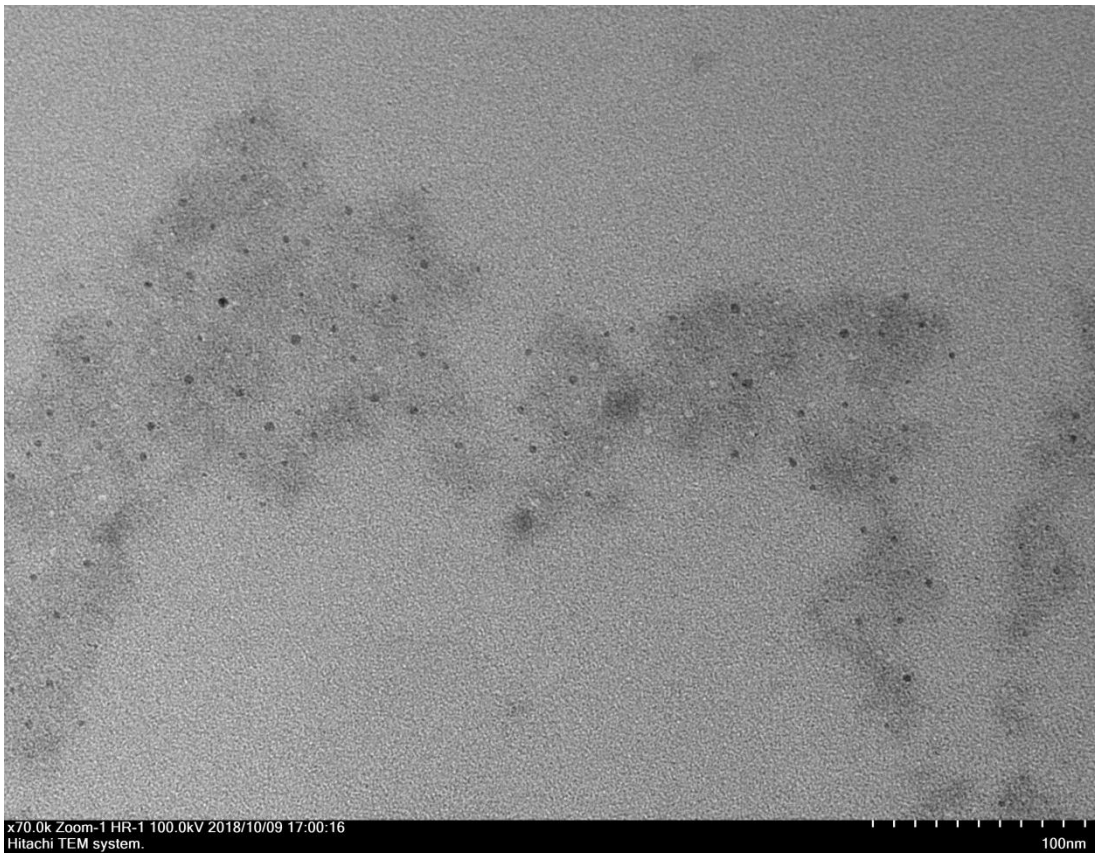

Figure S37. TEM image of palladium nanoparticles obtained at 2.0 h of Heck reaction with heterogeneous catalyst precursor. 70k magnification.

Figure S38. TEM image of palladium nanoparticles obtained at 4.0 h of Heck reaction with heterogeneous catalyst precursor. 70k magnification.

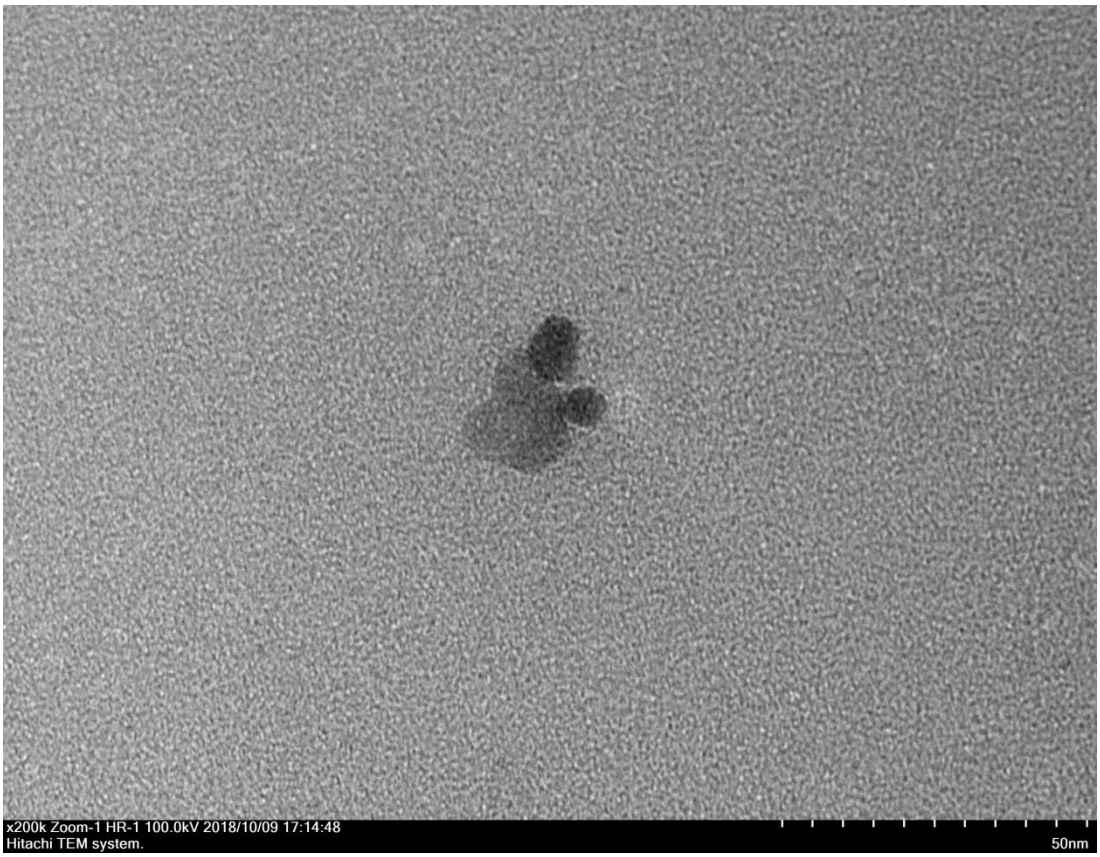

Figure S39. TEM image of palladium nanoparticles obtained at 4.0 h of Heck reaction with heterogeneous catalyst precursor. 200k magnification.

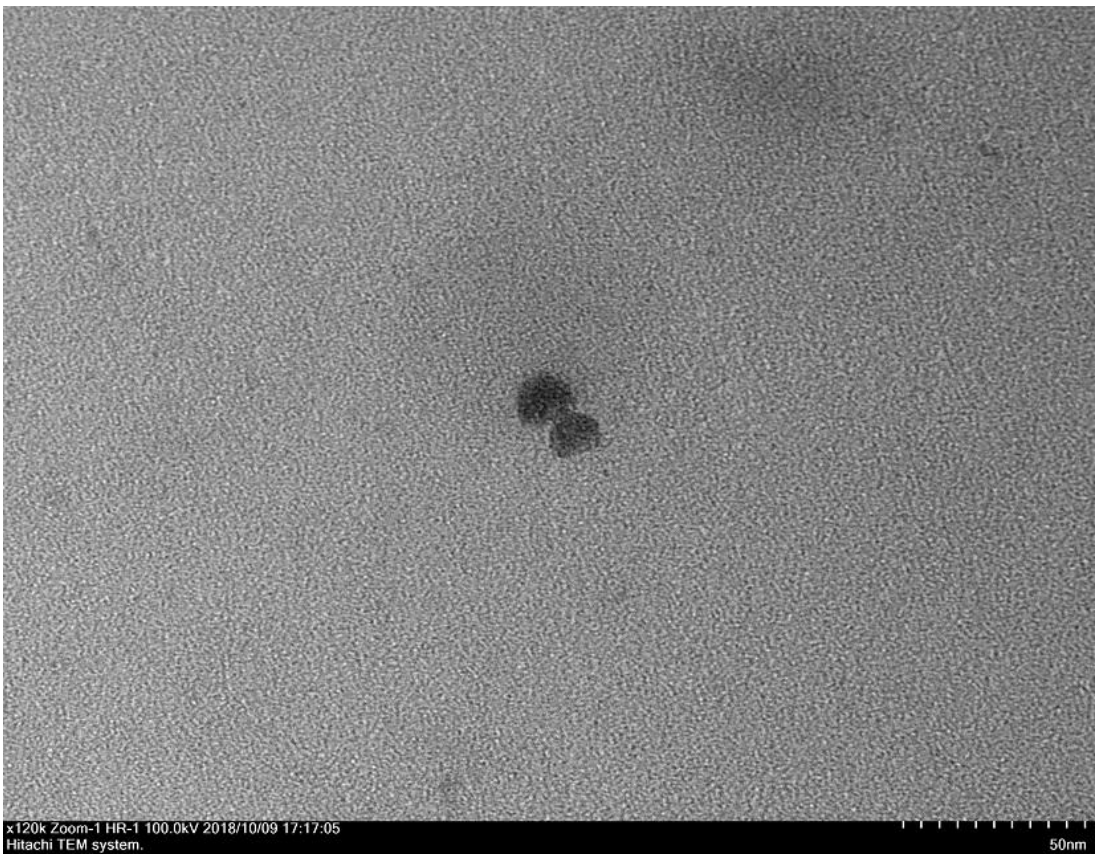

Figure S40. TEM image of palladium nanoparticles obtained at 4.0 h of Heck reaction with heterogeneous catalyst precursor. 120k magnification.

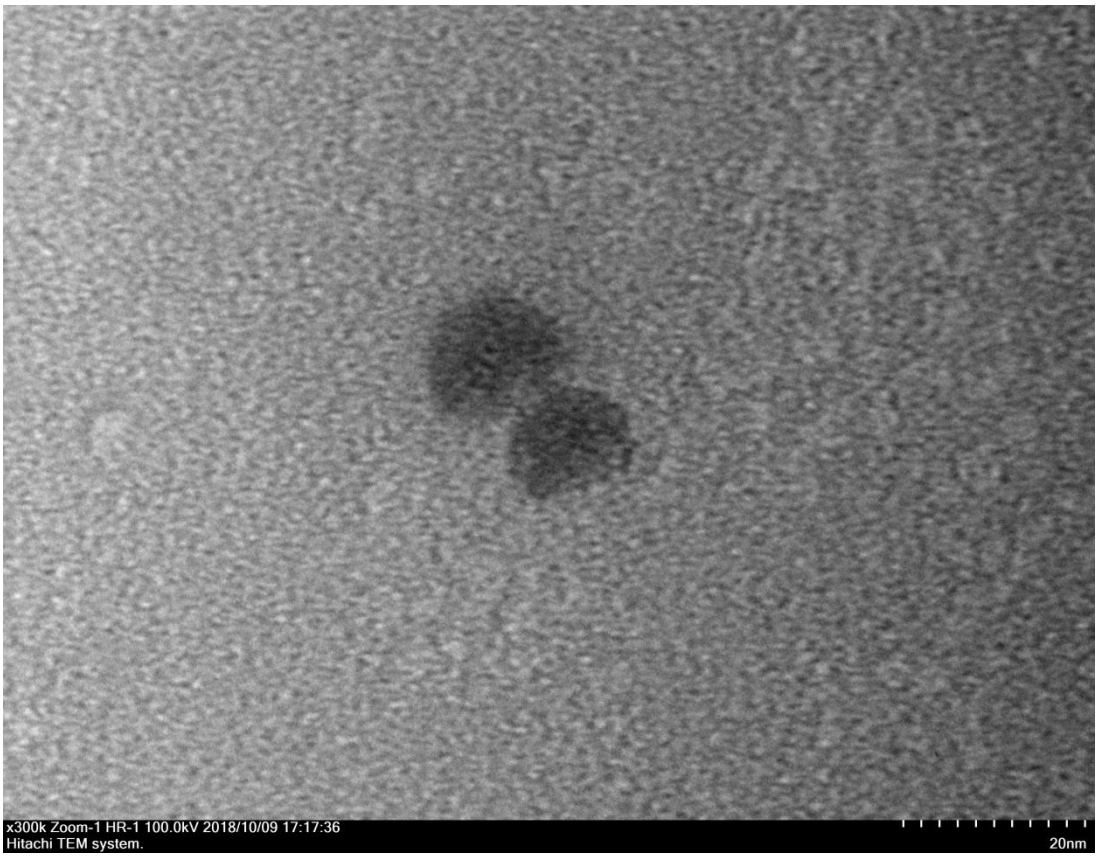

Figure S41. TEM image of palladium nanoparticles obtained at 4.0 h of Heck reaction with heterogeneous catalyst precursor. 300k magnification.

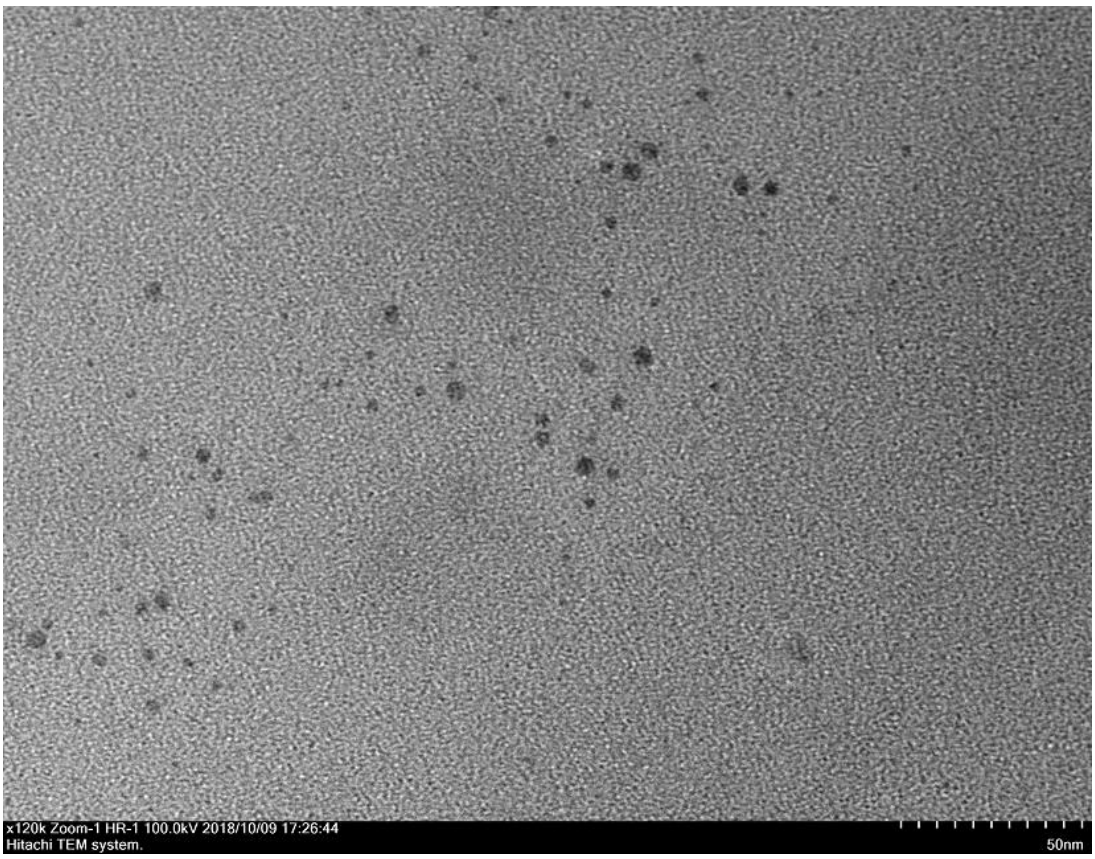

Figure S42. TEM image of palladium nanoparticles obtained at 4.0 h of Heck reaction with heterogeneous catalyst precursor. 120k magnification.

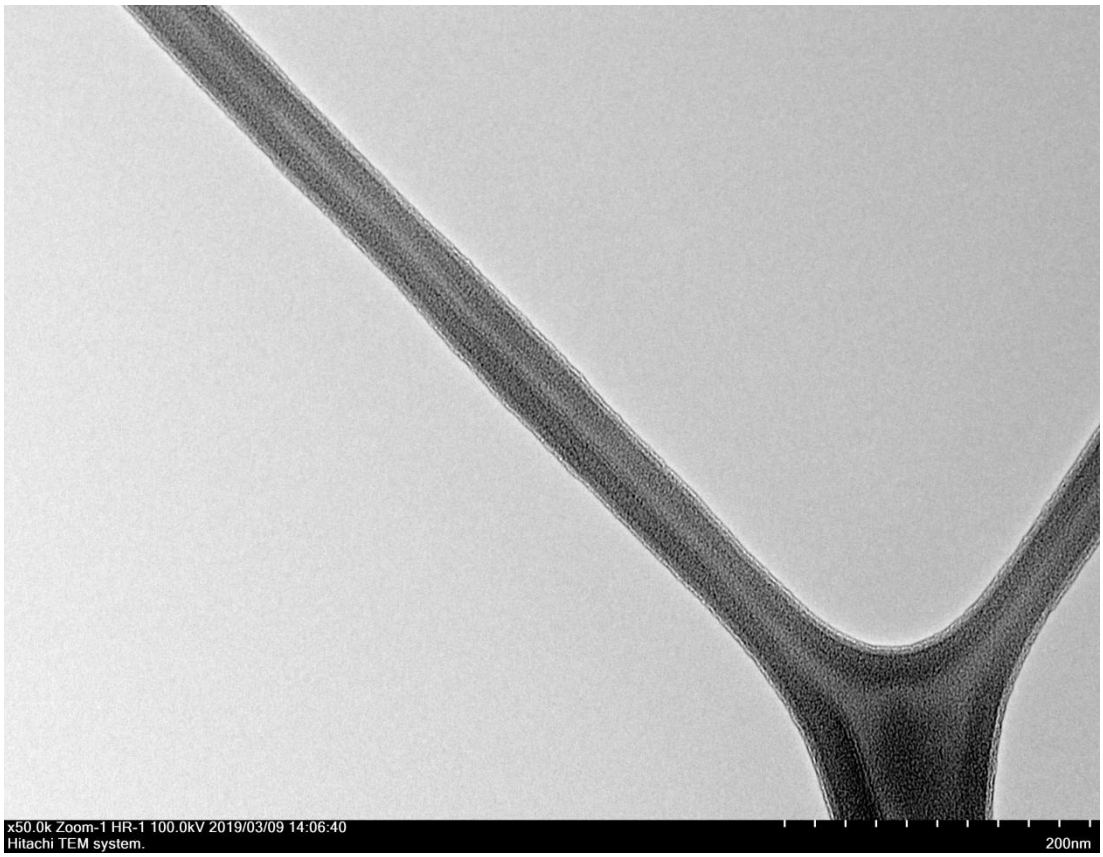

Figure S43. TEM image of the grid surface at the initial moment of Heck reaction with homogeneous catalyst precursor. 50k magnification.

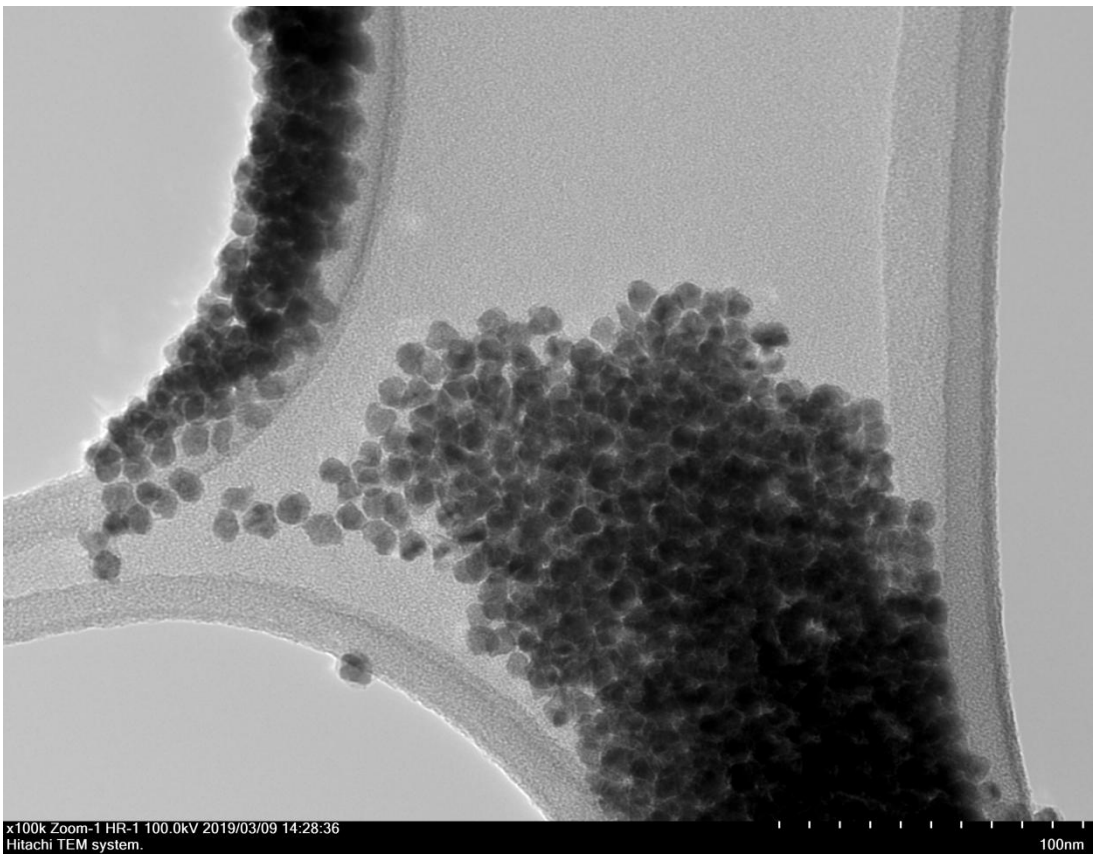

Figure S44. TEM image of palladium nanoparticles obtained at 5 min of Heck reaction with homogeneous catalyst precursor. 100k magnification.

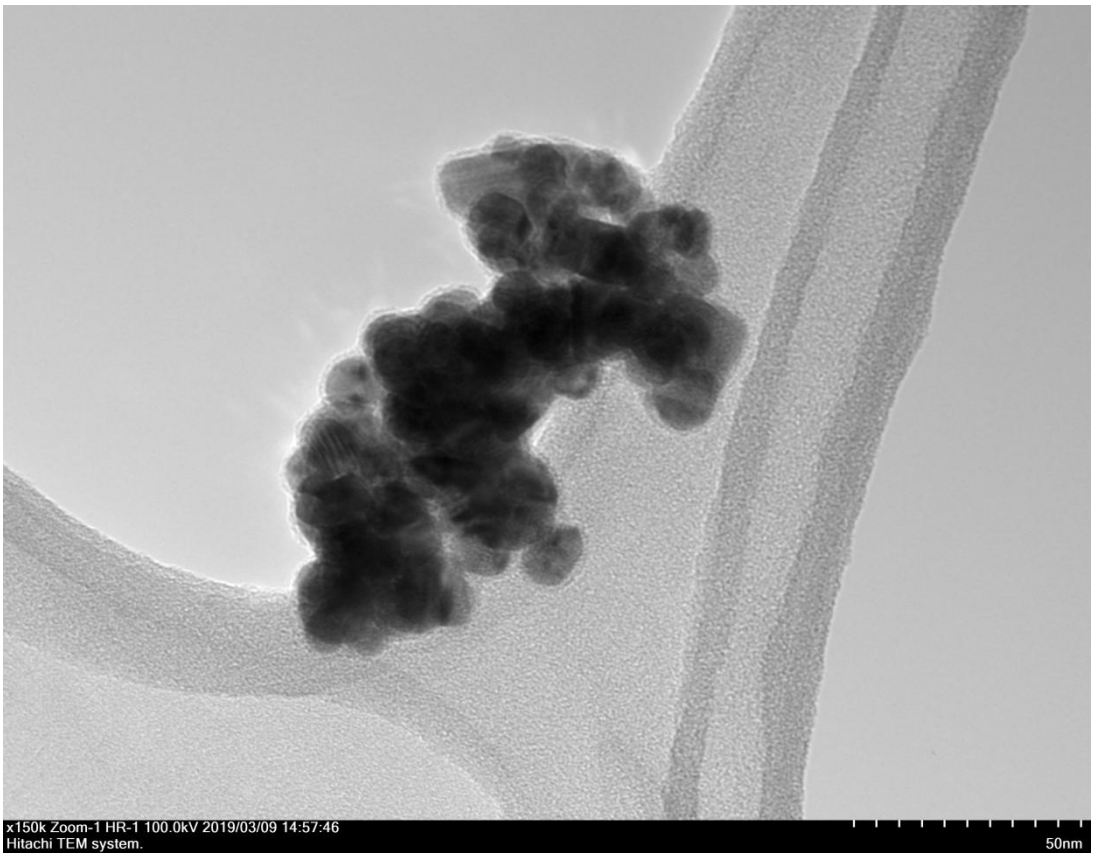

Figure S45. TEM image of palladium nanoparticles obtained at 15 min of Heck-reaction with homogeneous catalyst precursor. 150k magnification.

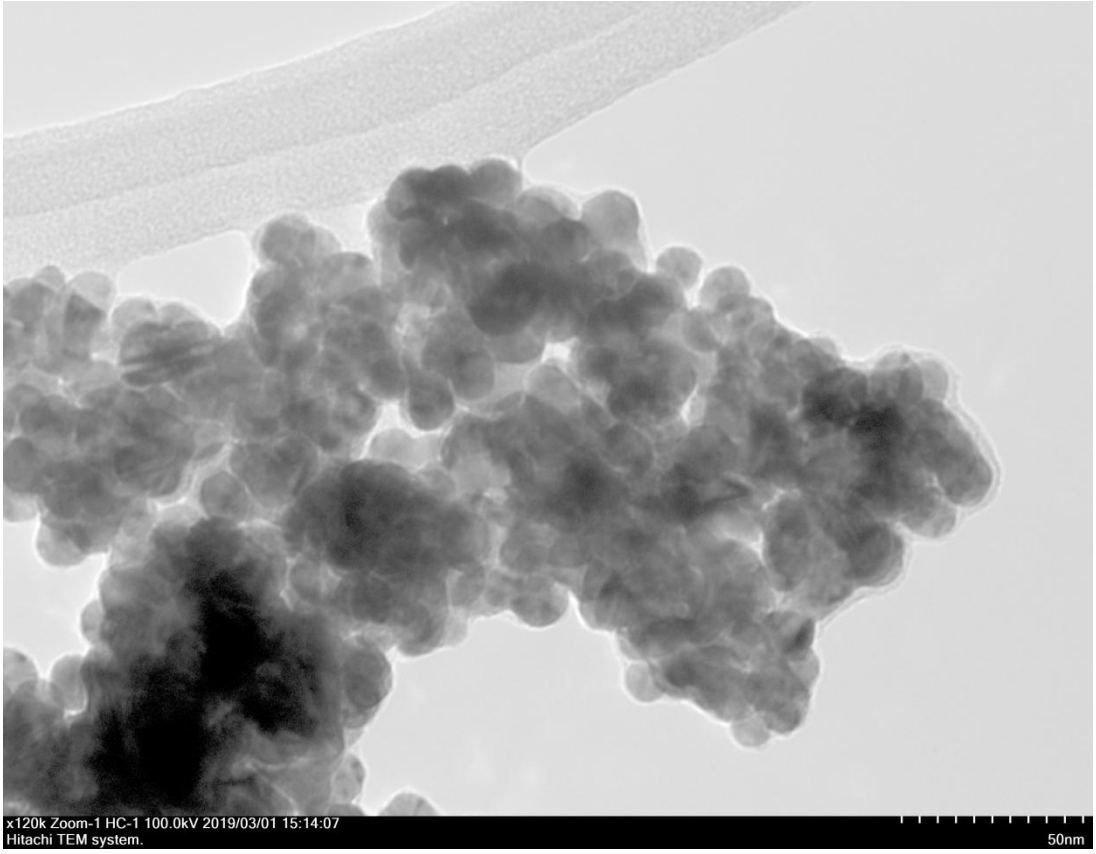

Figure S46. TEM image of palladium nanoparticles obtained at 30 min of Heck reaction with homogeneous catalyst precursor. 120k magnification.

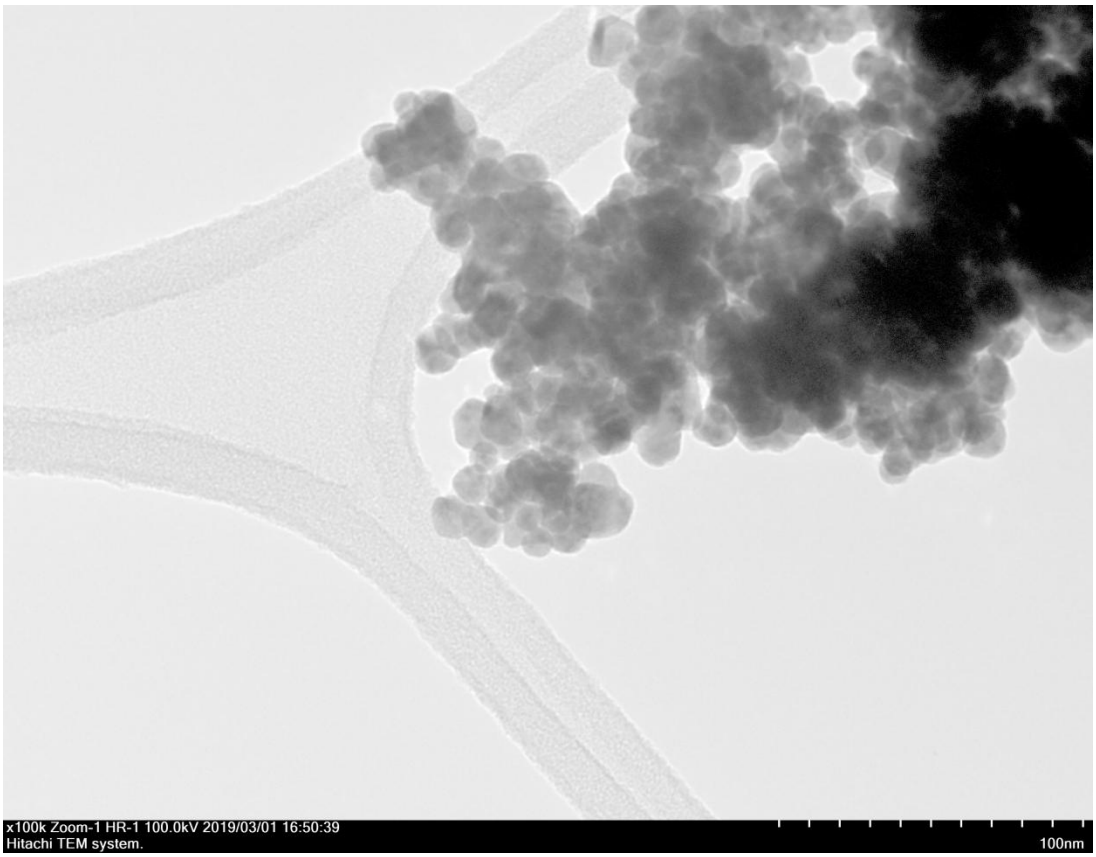

Figure S47. TEM image of palladium nanoparticles obtained at 30 min of Heck-reaction with homogeneous catalyst precursor. 100k magnification.

S7. XPS-spectra

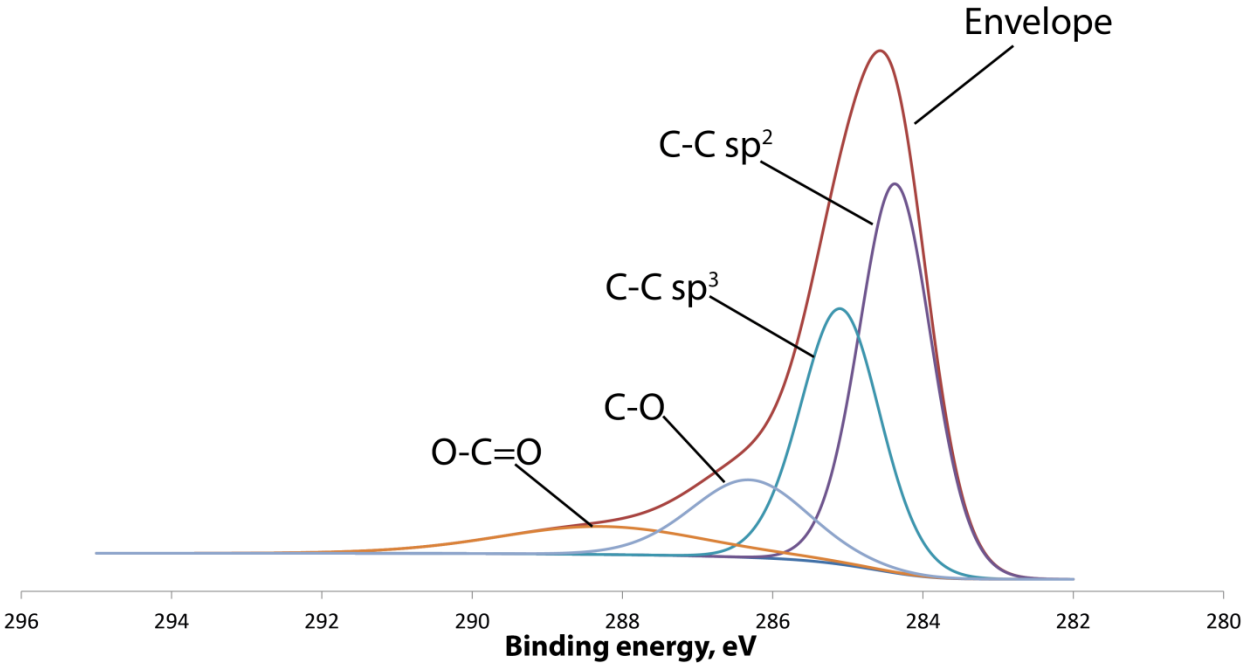

Figure S48. XPS-spectra of the pure carbon film on a carbon coated copper grid for TEM.

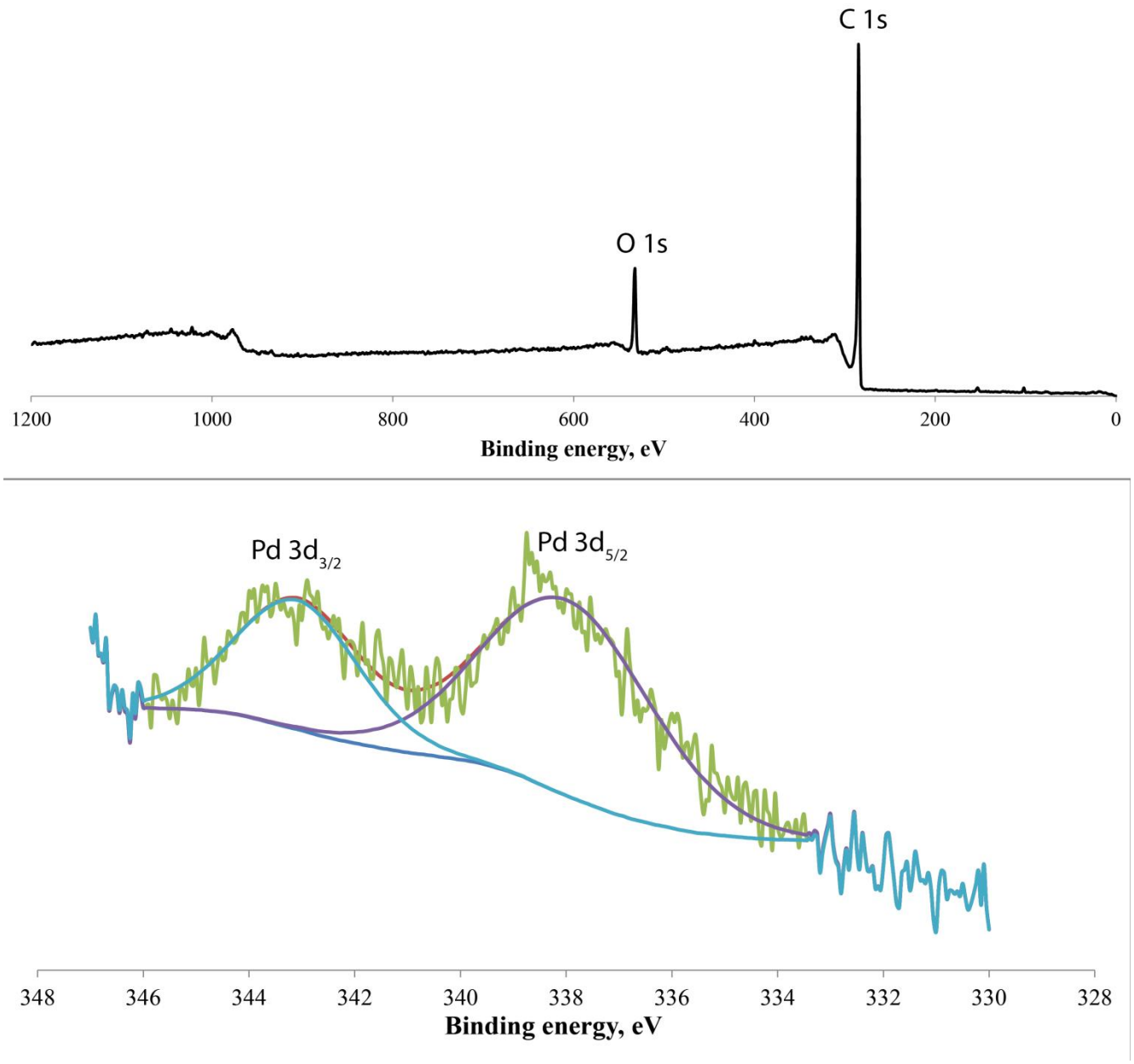

Figure S49. XPS-spectra of a carbon coated copper grid with Pd NPs formed according by Method A in the absence of ligands.

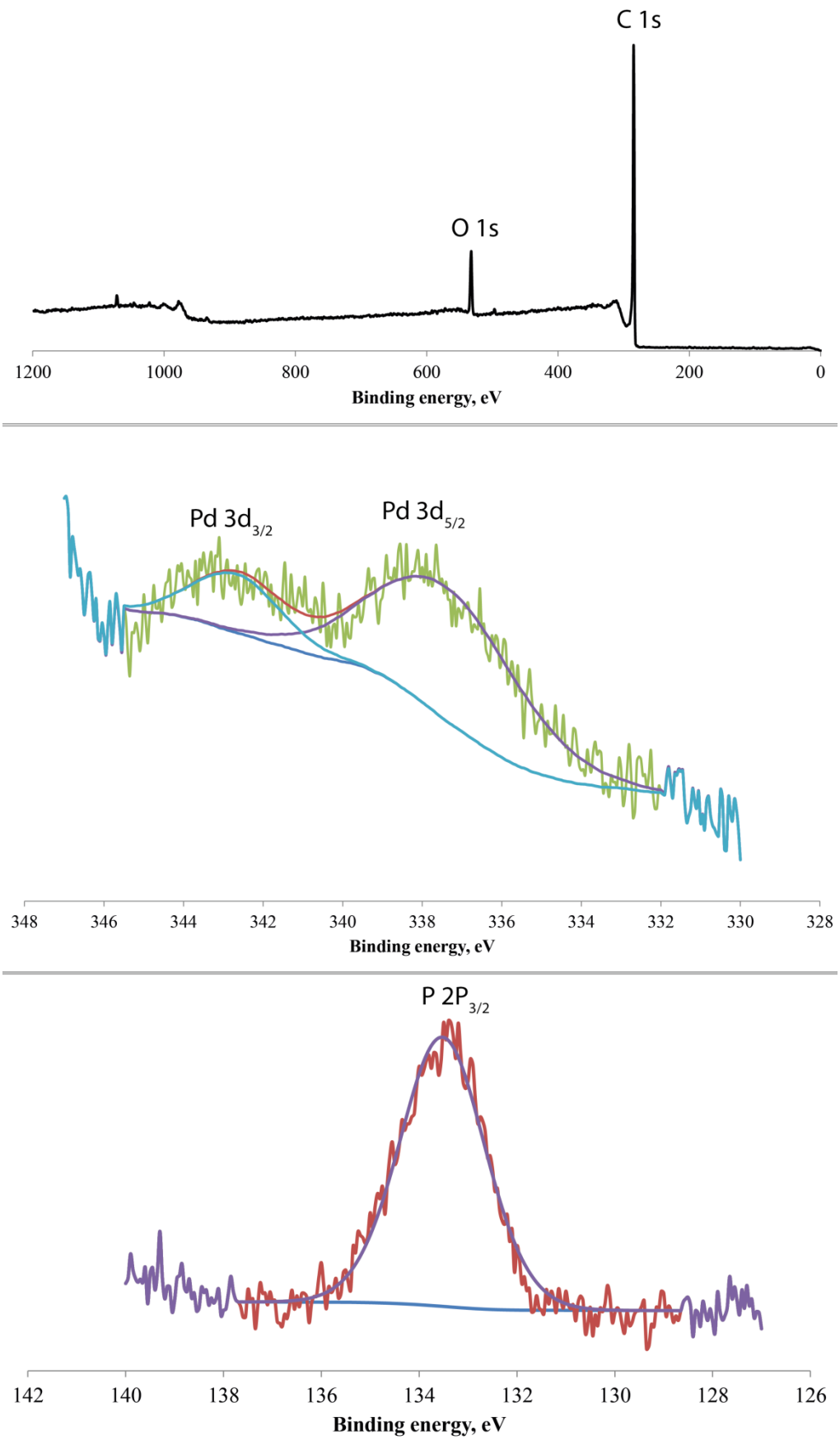

Figure S50. XPS-spectra of a carbon coated copper grid with Pd NPs formed by Method A in the presence of tris-(4-chlorophenyl)phosphine.

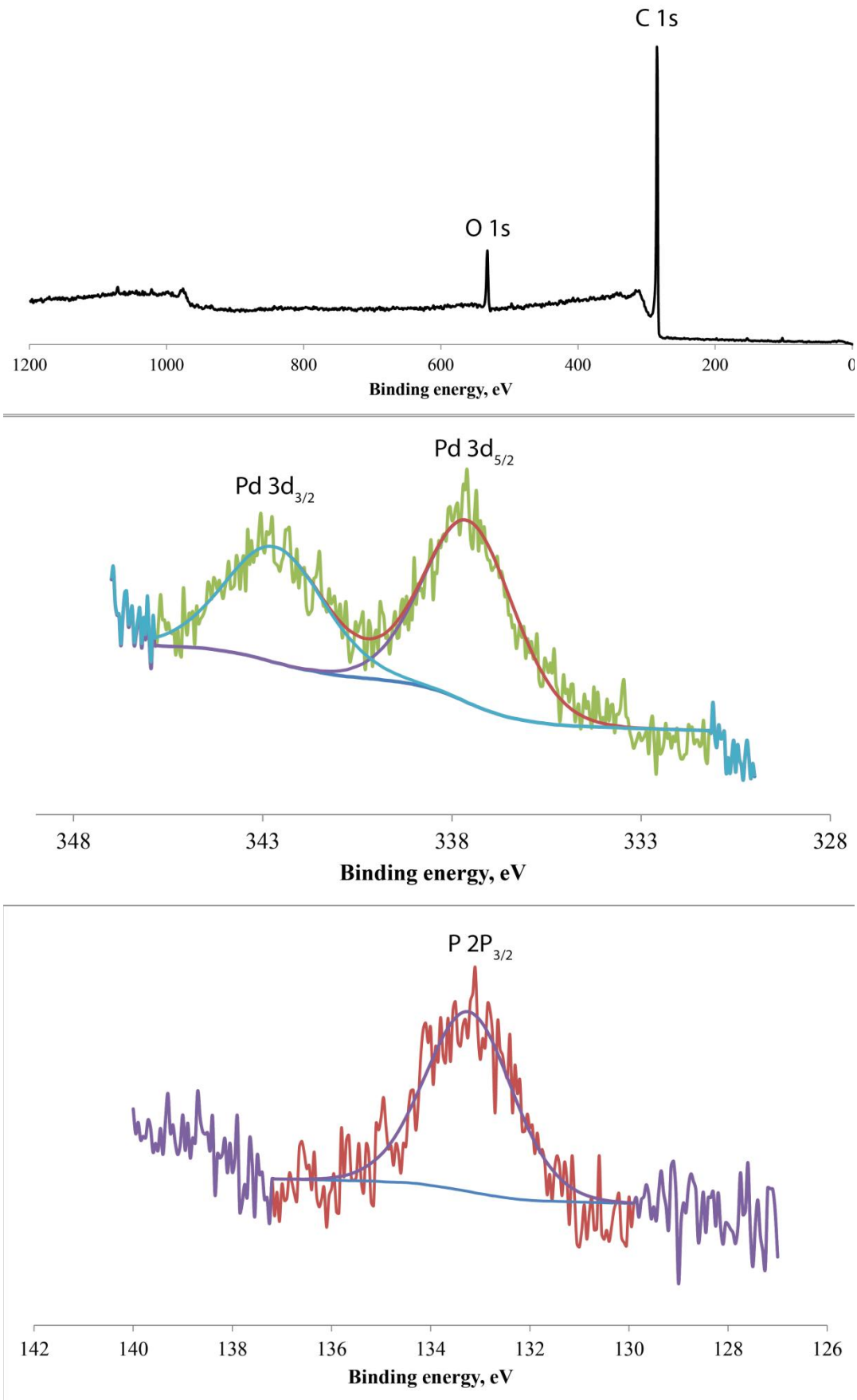

Figure S51. XPS-spectra of a carbon coated copper grid with Pd NPs formed by Method A in the presence of DPPM.

Table S2. Composition of a carbon coated copper grid with palladium nanoparticles as determined by XPS.

	C	Pd	O	P
Without a ligand	92.00 %	0.08 %	7.92 %	–
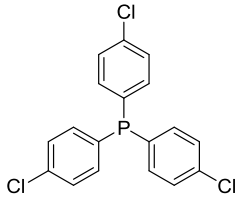 Tris-(4-chlorophenyl)phosphine	92.09 %	0.12 %	7.67 %	0.12 %
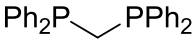 DPPM	92.07 %	0.06 %	7.69 %	0.18 %

S8. TEM-EDX of Pd nanoparticles

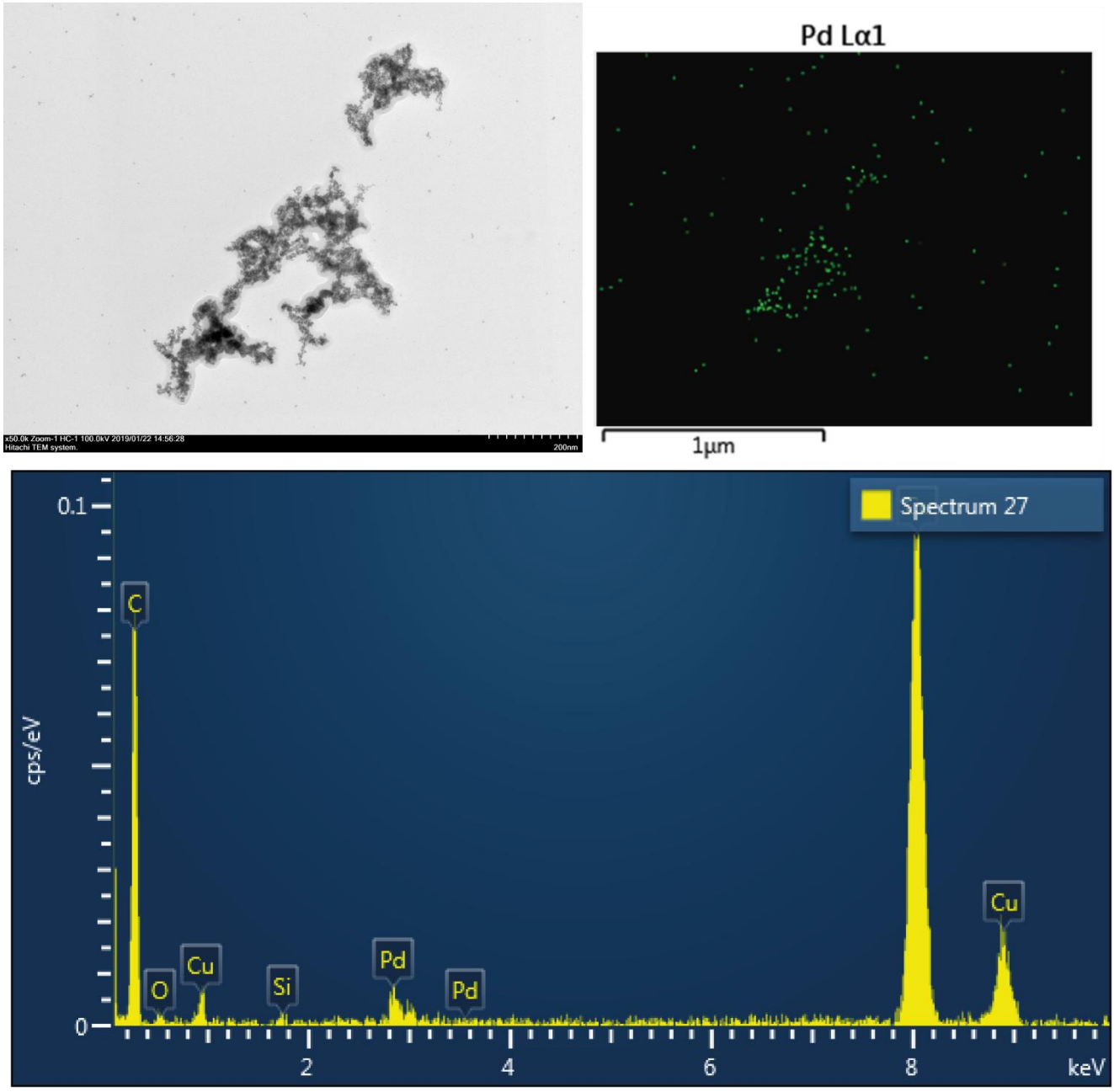

Figure S52. TEM-EDX of Pd NPs obtained by Method A.

S9. Liquid-phase FE-SEM

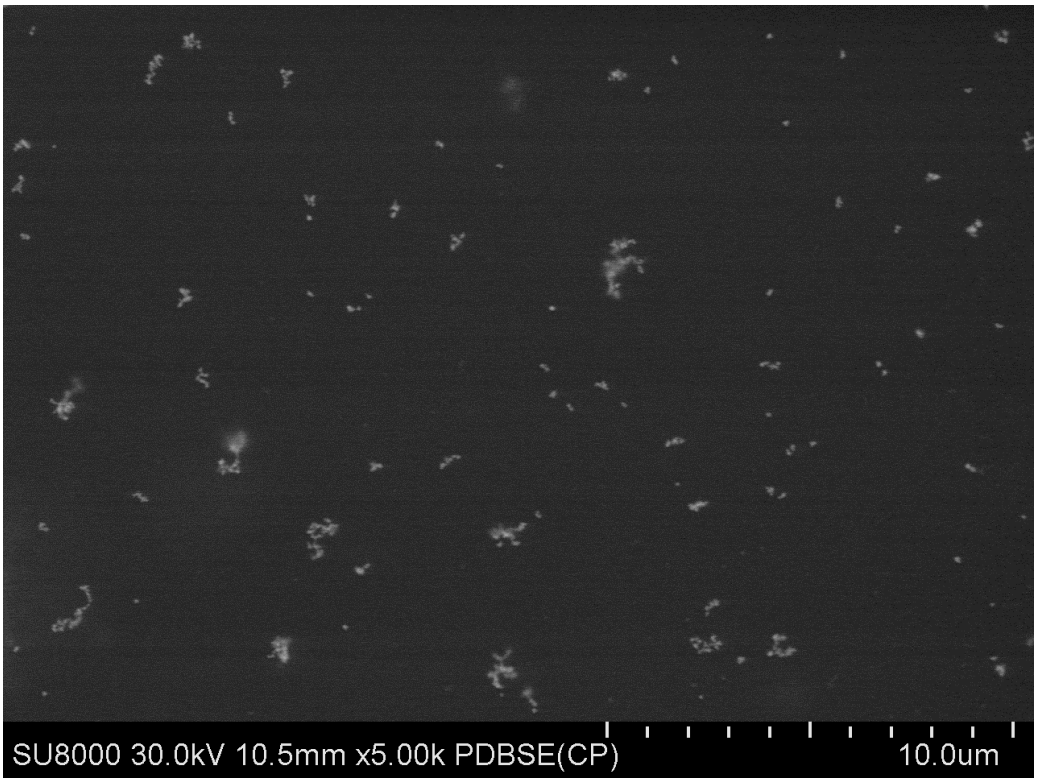

Figure S53. Liquid-phase FE-SEM image of the Pd-containing colloid prepared by heating of $Pd(OAc)_2$ in NMP in the presence of iodobenzene (5k magnification).

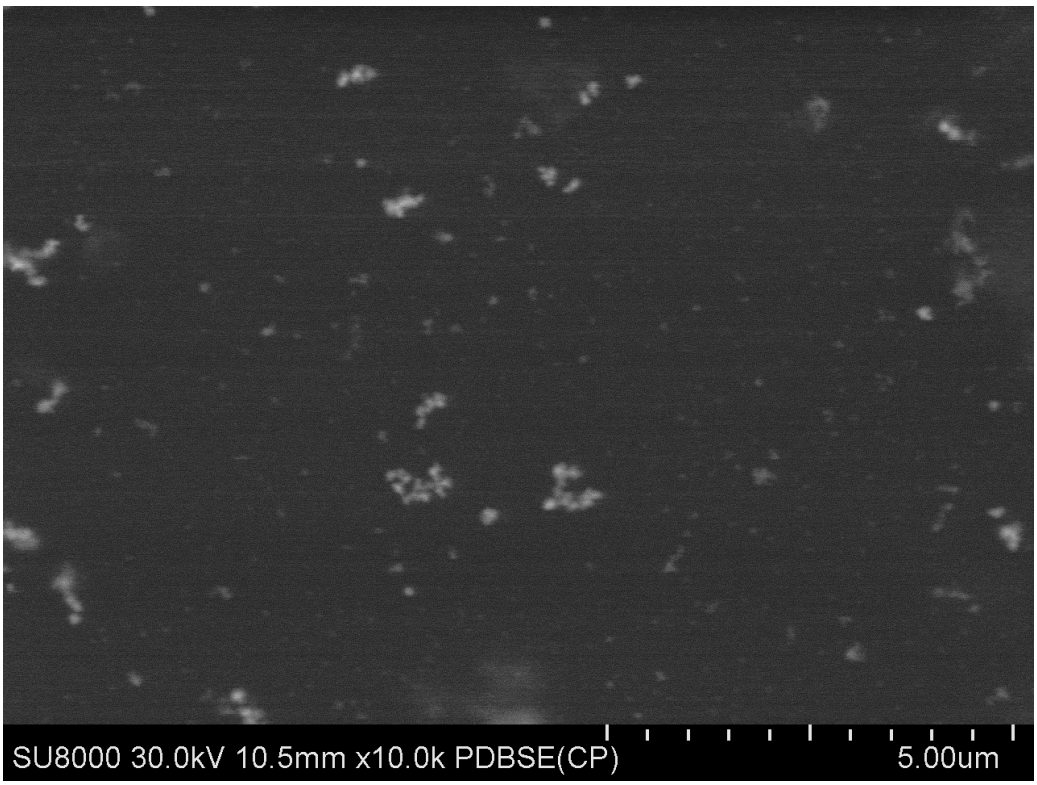

Figure S54. Liquid-phase FE-SEM image of the Pd-containing colloid prepared by heating of $Pd(OAc)_2$ in NMP in the presence of iodobenzene (10k magnification).

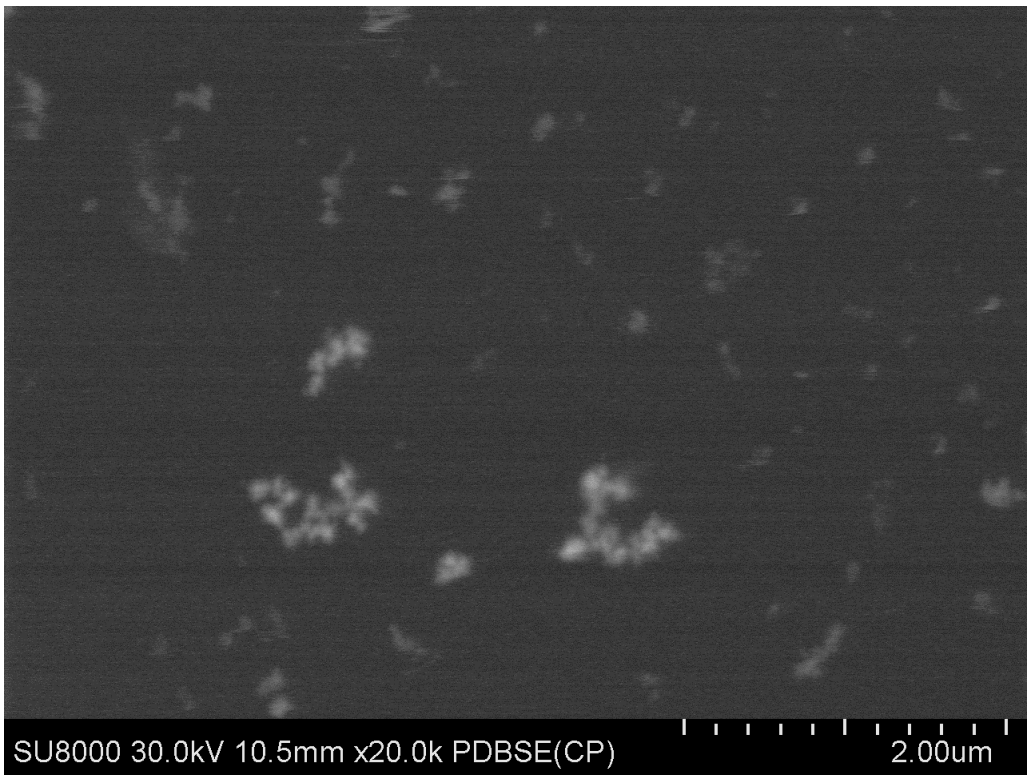

Figure S55. Liquid-phase FE-SEM image of the Pd-containing colloid prepared by heating of $Pd(OAc)_2$ in NMP in the presence of iodobenzene (20k magnification, enlarged version of image from the main text of the article).

S10. TEM image of Pd-containing species from $Pd(OAc)_2$ in NMP and PhI

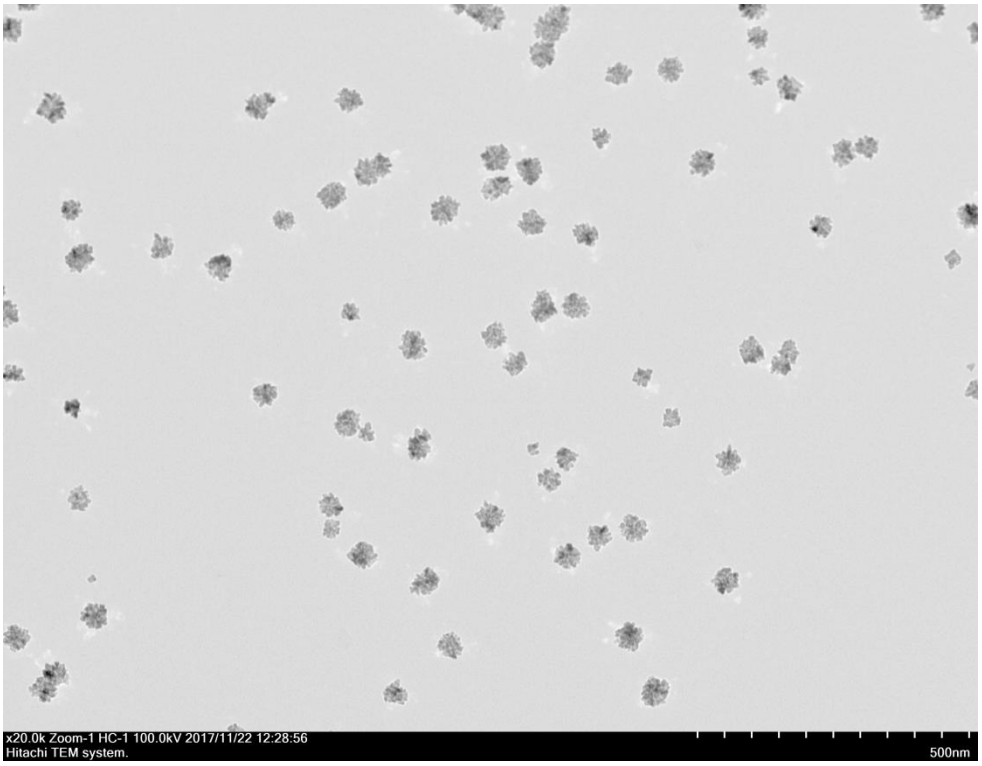

Figure S56. TEM image of Pd-containing species trapped from the colloid prepared by heating of $Pd(OAc)_2$ in NMP in the presence of iodobenzene (20k magnification).

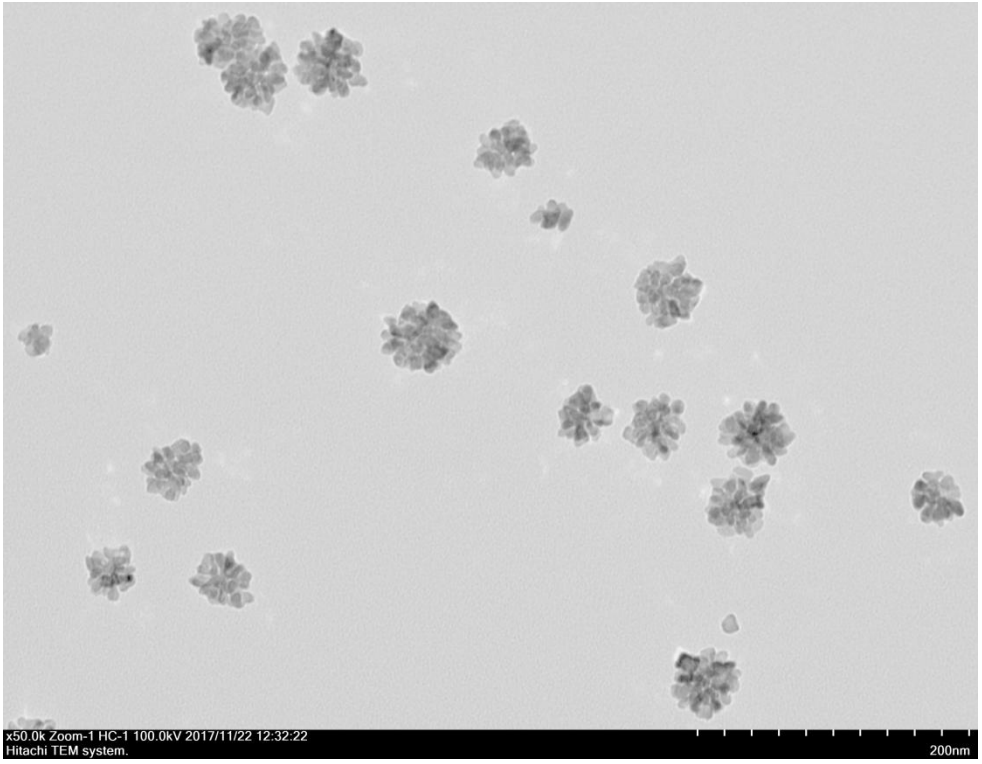

Figure S57. TEM image of Pd-containing species trapped from the colloid prepared by heating of $Pd(OAc)_2$ in NMP in the presence of iodobenzene (50k magnification, enlarged version of image from the main text of the article).

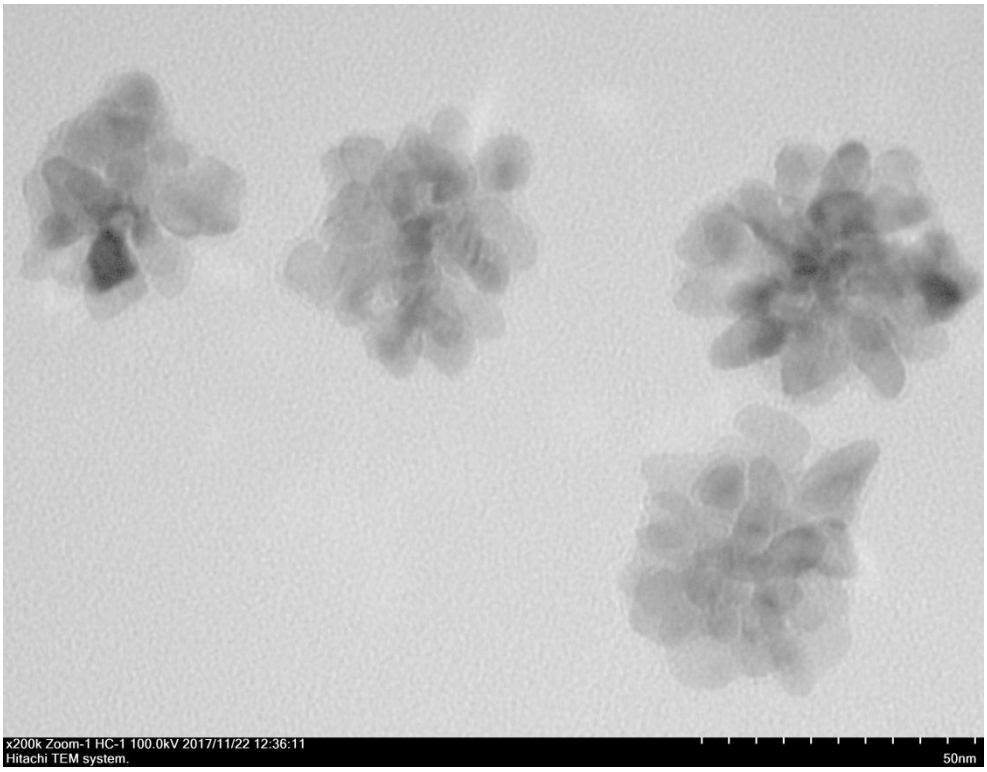

Figure S58. TEM image of Pd-containing species trapped from the colloid prepared by heating of $Pd(OAc)_2$ in NMP in the presence of iodobenzene (200k magnification, enlarged version of image from the main text of the article).

S11. EXAFS data

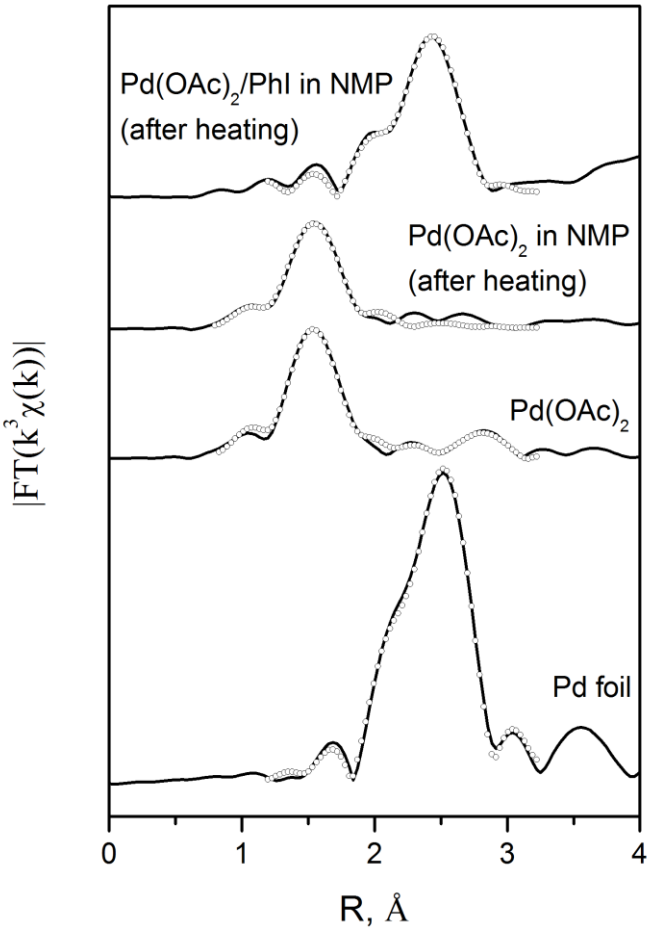

Figure S59. Fourier transforms of Pd K-edge EXAFS spectra of the samples under investigation: liquid systems prepared by the heating of palladium acetate solution in NMP in the presence and in the absence of iodobenzene; samples of palladium foil and solid palladium acetate as standards. Experimental curves (solid lines) and best fits (dots).

Table S3. Parameters of the local environment of Pd atoms in the samples studied from EXAFS data analysis (fitting ranges: R=1.2-3.2 Å; k=2.0-12.5 $Å^{-1}$).

Sample	R_f	ΔE, eV	Path	N	R, Å	σ^2, $Å^2$
Pd foil	0.004	2.5	Pd-Pd	12	2.75	0.0049
$Pd(OAc)_2$ (1 sphere)	0.068	6.0	Pd-O	4	2.01	0.0023
$Pd(OAc)_2$ (trimer)	0.012	6.2	Pd-O Pd...C Pd…Pd Pd…O	4 4 2 4	2.01 3.00 3.22 3.21	0.0023 0.0032 0.0139 0.0046
$Pd(OAc)_2$ in NMP (1 sphere)	0.030	7.1	Pd-O	3.3	2.02	0.0022
$Pd(OAc)_2$/PhI in NMP	0.003	-0.8	Pd-I Pd-Pd	2.4 3.5	2.59 2.75	0.0024 0.0028